

# Infrared quasi-fixed solutions in the NMSSM

R. B. Nevzorov and M. A. Trusov  
*ITEP, Moscow, Russia*

October 30, 2018

## Abstract

The considerable part of the parameter space in the MSSM corresponding to the infrared quasi fixed point scenario is almost excluded by LEP II bounds on the lightest Higgs boson mass. In the NMSSM the mass of the lightest Higgs boson reaches its maximum value in the strong Yukawa coupling limit when Yukawa couplings are essentially larger than gauge ones at the Grand Unification scale. In this limit the solutions of the renormalisation group equations are attracted to the infrared and Hill type effective fixed lines or surfaces in the Yukawa coupling parameter space. They are concentrated in the vicinity of quasi fixed points for  $Y_i(0) \rightarrow \infty$ . However the solutions are attracted to such points rather weakly. For this reason when all  $Y_i(0) \sim 1$  the solutions of the renormalisation group equations are gathered near a line in the Hill type effective surface. In the paper the approximate solutions for the NMSSM Yukawa couplings are given. The possibility of  $b$ -quark and  $\tau$ -lepton Yukawa coupling unification at the scale  $M_X$  is also discussed.

# 1 Introduction

The existence of quasi-fixed points is among the most spectacular and the most interesting properties of renormalization group equations. A feature characteristic to those solutions to renormalization group equations that approach such points is that a number of fundamental parameters of the theory are focused in a narrow interval in the infrared region. This means that, at the electroweak scale, some constants or their combinations cease to depend on the boundary conditions. That solutions to renormalization group equations behave in so peculiar a way in the vicinities of quasi-fixed points results in that the parameter space of the theory being considered is constrained for a wide class of such solutions. As a result, the predictive power of the theories being discussed becomes higher near these points. Nonetheless, it turns out that, within the minimal Standard Model (SM), the quasi-fixed point scenario leads to overly high a value for the mass of the  $t$ -quark, which contradicts experimental data obtained at FNAL.

In contrast to the SM, its supersymmetric (SUSY) generalization – the Minimal SUSY Standard Model (MSSM) – features two Higgs doublets (not one),  $H_1$  and  $H_2$ . Upon a spontaneous breakdown of symmetry, they develop nonzero vacuum expectation values  $v_1$  and  $v_2$ , with the constraint  $v^2 = v_1^2 + v_2^2 = (246 \text{ GeV})^2$  being satisfied. In relation to what occurs in the SM, the  $t$ -quark running mass  $m_t$  that is generated within SUSY models upon the breakdown of  $SU(2) \otimes U(1)$  gauge symmetry involves an additional factor  $\sin \beta$ ,

$$m_t(M_t^{\text{pole}}) = \frac{h_t(M_t^{\text{pole}})}{\sqrt{2}} v \sin \beta, \quad (1)$$

where  $\tan \beta = v_2/v_1$  and  $h_t$  is the Yukawa coupling constant for the  $t$ -quark. Since  $\sin \beta \leq 1$ ,  $m_t(M_t^{\text{pole}})$  is always less in the MSSM than in the SM at the same values of the Yukawa coupling constants. Recent experimental data on the  $t$ -quark mass make it possible to determine  $m_t(M_t^{\text{pole}})$  within the  $\overline{MS}$  scheme [1]. It proves to be  $m_t(M_t^{\text{pole}}) = 165 \pm 5 \text{ GeV}$ . The uncertainty in the determination of the running mass of the  $t$ -quark stems predominantly from the experimental error with which its pole mass was measured ( $M_t^{\text{pole}} = 174.3 \pm 5.1 \text{ GeV}$  [2]).

Equation (1) unambiguously relates  $\tan \beta$  to the value of the Yukawa coupling constant for the  $t$ -quark at the electroweak scale. At modest values of  $\tan \beta$  ( $\tan \beta \ll 50 - 60$ ), the Yukawa coupling constants for the  $b$ -quark,  $h_b$ , and for the  $\tau$ -lepton,  $h_\tau$ , are negligibly small, which makes it possible to obtain an analytic solution to the renormalization group equation within the MSSM [3]. In this case, the boundary conditions are imposed at the scale  $M_X \approx 3 \cdot 10^{16} \text{ GeV}$ , where the gauge coupling constants are naturally unified within the MSSM. For the  $t$ -quark Yukawa coupling constant, it is convenient to represent an exact solution to the renormalization group equations in the form

$$Y_t(t) = \frac{\frac{E(t)}{6F(t)}}{1 + \frac{1}{6Y_t(0)F(t)}}, \quad (2)$$

where  $Y_t(t) = h_t^2(t)/(4\pi)^2$  and  $t = \ln(M_X^2/q^2)$ . The explicit expressions for the functions  $E(t)$  and  $F(t)$  are presented in the Appendix (see (27)). At the electroweak scale, the

second term in parentheses is much less than unity for  $h_t^2(0) \geq 1$ . The dependence of  $h_t^2(t)$  on the initial conditions at  $t = 0$  is weak, and the relevant solution to the renormalization group equations approaches a quasi-fixed point [4]:  $Y_{\text{QFP}}(t) = E(t)/6F(t)$ . Formally, a solution of this type can be obtained by making  $Y_t(0)$  tend to infinity in expression (2). The situation here is, however, different from that near the Pendleton–Ross infrared fixed point [5]–[8], which solutions to the renormalization group equations approach only in the asymptotic regime for  $q^2 \rightarrow 0$ : the deviation from  $Y_{\text{QFP}}$  at finite values of  $Y_t(0)$  is determined by the ratio  $Y_{\text{QFP}}(t)/(E(t)Y_t(0))$ , which is of order  $1/(10h_t^2(0))$  at the electroweak scale and which is small at comparatively large  $h_t^2(0)$  ( $h_t^2(0) \geq 1$ ). For a wide class of solutions, this interesting property of the renormalization group equations within the MSSM makes it possible to predict quite precisely the value of the Yukawa coupling constant for the  $t$ -quark at the scale  $q = M_t^{\text{pole}}$ ,

$$h_{\text{QFP}}^2(t_0) = 0.87 \cdot g_3^2(t_0) = 1.26, \quad (3)$$

where  $g_3$  is the gauge coupling constant for strong interaction and  $t_0 = 2 \ln(M_X/M_t^{\text{pole}})$ . The accuracy of this prediction becomes higher with increasing  $h_t^2(0)$ . At sufficiently large initial values of  $Y_t(t)$ , it would be illegitimate to restrict the analysis to one-loop renormalization group equations – it is necessary to take into account higher order perturbative corrections. Moreover, the value of the Yukawa coupling constant for the  $t$ -quark at the electroweak scale depends on the strong interaction coupling constant, which we set to  $\alpha_3(M_Z) = 0.118$ . Nevertheless, all these uncertainties do not lead to significant deviation from (3). By way of example, we indicate that the calculations that were performed in [9] and which employed the four-loop beta function showed that deviations from (3) are within 2%.

For each fixed value of  $Y_t(0)$ , the Yukawa coupling constant for the  $t$ -quark at the electroweak scale can be evaluated by using the exact analytic solution (2), whereupon  $\tan \beta$  can be determined by substituting the resulting value of  $h_t(t_0)$  into (4). The theoretical analysis performed in [10]–[13] revealed that, for the renormalization group equations within the MSSM, a broad class of solutions corresponding to the infrared quasi-fixed point regime leads to  $\tan \beta$  values ranging between 1.3 and 1.8. With increasing Yukawa coupling constant for the  $t$ -quark, the corresponding trilinear coupling constant  $A_t$  for the interaction of scalar particles and the combination  $\mathfrak{M}_t^2 = m_Q^2 + m_U^2 + m_2^2$  of the scalar particle masses cease to depend on the initial conditions. In the vicinity of the quasi-fixed point, they are expressed in terms of only the gaugino mass at the scale  $M_X$ , with the result that the parameter space is further constrained. In the infrared quasi-fixed point regime at  $\tan \beta \sim 1$ , the properties of solutions to the set of renormalization group equations and the spectrum of particles were investigated in [8], [12]–[16].

Finally, there is yet another circumstance that appears as an incentive to study the limit of strong Yukawa coupling within the MSSM. Minimal schemes that are used to unify gauge interactions and which are based on gauge groups like  $SU(5)$ ,  $E_6$ , or  $SO(10)$  predict the equality of the Yukawa coupling constants  $h_b$  and  $h_\tau$  for , respectively, the  $b$ -quark and the  $\tau$ -lepton at the scale  $M_X$  [17]. Within the MSSM,  $h_b$  and  $h_\tau$  are unified at two specific values of  $h_t(M_t^{\text{pole}})$ . One of these fails within a narrow region near  $h_{\text{QFP}}(t_0)$ , while the other corresponds to the scenario of large  $\tan \beta$ . In more detail, the problem of  $b - \tau$  unification within the MSSM was discussed in [7], [15],[16],[18],[19],[20].

The spectrum of the Higgs sector of the MSSM contains four massive states: two CP-odd states, one CP-even state, and one charged state. The presence of a light Higgs boson

in the CP–even sector is an important feature of SUSY models. The upper limit on its mass greatly depends on  $\tan\beta$ . A reduction of the number of independent parameters in the infrared quasi–fixed point regime made it possible to determine, to a sufficiently high degree of precision, an upper limit on the mass of the lightest CP–even Higgs boson. In the case being considered, comparatively small values of  $\tan\beta$  result in that its mass does not exceed  $94 \pm 5$  GeV [11]-[13]. This limit is 25 – 30 GeV lower than the absolute upper limit in the minimal SUSY model. At the same time the lower limit on the mass of the lightest Higgs boson from LEP II data – in the case of a heavy spectrum of SUSY particles, it coincides with the corresponding limit on the Higgs boson mass in the SM – is 113.3 GeV [21]. Actually, this means that a major part of solutions approaching the infrared quasi–fixed point within the MSSM have already been ruled out by the existing LEP II data. In order to meet the experimental constraints on the mass of the lightest Higgs boson, it is necessary either to go over to studying solutions that lead to large values of  $\tan\beta$  within the MSSM or to extend the Higgs sector of the minimal SUSY model. The detailed investigations that were performed in [13], [16], [19], [22] revealed that, at  $\tan\beta \approx 50 - 60$ , solutions to the renormalization group equations also approach the infrared quasi–fixed point, the basic properties of the solutions remaining unchanged.

The nonminimal SUSY SM (NMSSM) [23]-[25] whose Higgs sector contains, in addition to the doublets  $H_1$  and  $H_2$ , an extra superfield  $Y$  that is a singlet with respect to  $SU(2) \otimes U(1)$  gauge interactions is the simplest extension of the MSSM. In the parameter space of the NMSSM, the region that corresponds to the limit of strong Yukawa coupling, in which case the Yukawa coupling constants  $Y_i(0)$  at the Grand Unification scale  $M_X$  are much greater than the gauge coupling constant  $\tilde{\alpha}(0)$ , is that which is the most appealing from the point of view of a theoretical analysis. It is the region where the upper limit on the mass of the lightest Higgs boson takes a maximum value that is few GeV greater than the corresponding absolute limit within the MSSM [26]. Moreover, it is possible, in the case being considered, to choose coupling constants in such a way as to obtain the unification of the Yukawa coupling constants for the  $b$ -quark and the  $\tau$ -lepton at the scale  $M_X$ .

For the Yukawa coupling constants in the limit of strong Yukawa coupling, we study here basic properties of solutions to the renormalization group equations within the NMSSM. We show that, in the limit  $Y_i(0) \rightarrow \infty$ , all solutions in the nonminimal SUSY model are concentrated, as in the MSSM, near quasi–fixed points that arise as the result of intersections of Hill lines or surfaces with some invariant line in the space of Yukawa coordinates. However, the solution are rather weakly attracted to these points. For  $Y_i(0) \gg \tilde{\alpha}(0)$ , all solutions to the renormalization group equations are therefore nonuniformly distributed near Hill lines or surfaces. Approximate solutions to the set of nonlinear differential equations that describe the evolution of  $Y_i(t)$  within the NMSSM are presented in the Appendix. The approximate solutions that are obtained in the present study are compared with the results of numerical calculations within the nonminimal SUSY model.

## 2 Upper limit on the mass of the lightest Higgs boson and renormalisation group equations in the NMSSM

By construction, the superpotential of the NMSSM is invariant under the discrete transformations  $y'_\alpha = e^{2\pi i/3} y_\alpha$  of the  $Z_3$  group [24]. The term  $\mu(H_1 H_2)$  in the superpotential of the NMSSM does not satisfy this requirement. For this reason, an extra superfield  $Y$  that is a singlet with respect to  $SU(2) \otimes U(1)$  gauge interactions is introduced in the NMSSM. The superpotential of the Higgs sector of the NMSSM [23]-[25] has the form

$$W_h = \lambda Y(H_1 H_2) + \frac{\lambda'}{3} Y^3. \quad (4)$$

Upon a spontaneous breakdown of  $SU(2) \otimes U(1)$  symmetry, the field  $Y$  develops a nonzero vacuum expectation value ( $\langle Y \rangle = y/\sqrt{2}$ ) and there arises an effective  $\mu$ -term ( $\mu = \lambda y/\sqrt{2}$ ).

The introduction of the neutral field  $Y$  in the superpotential of the NMSSM leads to the emergence of the corresponding  $F$ -term in the potential of the interaction of Higgs fields. As a result, the upper limit on the mass of the lightest Higgs boson proves to be greater than in the MSSM. Specifically, we have

$$m_h \leq \sqrt{\frac{\lambda^2}{2} v^2 \sin^2 2\beta + M_Z^2 \cos^2 2\beta + \Delta_1 + \Delta_2}, \quad (5)$$

where  $\Delta_1$  and  $\Delta_2$  stand for, respectively, one-loop and two-loop corrections. At  $\lambda = 0$ , the expressions for the above upper limit within the MSSM and the NMSSM coincide. In the tree approximation, relation (5) was obtained in [25]. The inclusion of loop corrections to the effective potential of Higgs fields leads to a considerable growth of the upper limit on  $m_h$ . The main contributions to  $\Delta_1$  and  $\Delta_2$  come from loops involving a  $t$ -quark and its superpartners. In the leading approximation, the contribution of loop corrections to the upper limit on the Higgs boson mass within the NMSSM is approximately equal to that within the minimal SUSY model. In calculating the corrections  $\Delta_1$  and  $\Delta_2$  within the NMSSM, it is necessary, however, to replace the parameter  $\mu$  by  $\lambda y/\sqrt{2}$ . One-loop and two-loop corrections within the MSSM were studied in [27] and [28], respectively. In the leading approximation, these corrections are proportional to  $m_t^4$ ; they depend logarithmically on the scale of SUSY breaking,  $M_S = \sqrt{m_{\tilde{t}_1} m_{\tilde{t}_2}}$  ( $m_{\tilde{t}_1}$  and  $m_{\tilde{t}_2}$  are the masses of the superpartners of the  $t$ -quark), and are virtually independent on the choice of  $\tan \beta$ . The Higgs sector in the nonminimal SUSY model and one-loop corrections to this sector were studied in [29]-[31]. The possibility of a spontaneous CP-violation in the Higgs sector of the NMSSM was considered in [31],[32]. In [33], the upper limit on the mass of the lightest Higgs boson within the NMSSM was compared with the corresponding limits within the minimal SM and minimal SUSY models. The most recent investigations revealed that, in the nonminimal SUSY model,  $m_h$  does not exceed 135 GeV [26].

From relation (5), it follows that the upper limit on  $m_h$  grows with the increasing  $\lambda(t_0)$ . It should be emphasised that only in the region of small  $\tan \beta$  is this limit markedly different from the corresponding limit within the MSSM. At large values of this parameter ( $\tan \beta \gg 1$ ), the quantity  $\sin 2\beta$  vanishes, so that the upper limits on the mass of the lightest Higgs boson within the MSSM and the NMSSM virtually coincide. But only in

the case of sufficiently large  $h_t(t_0)$  is the scenario of small  $\tan\beta$  realised,  $\tan\beta$  becoming smaller with increasing  $h_t(t_0)$ , as can be seen from relation (1). At the same time, an analysis of the renormalisation group equations within the MSSM and the NMSSM reveals that the growth of the Yukawa coupling constants at the electroweak scale is accompanied by an increase in  $h_t(0)$  and  $\lambda(0)$  at the Grand Unification scale. Thus, it becomes clear that the upper limit on the mass of the lightest Higgs boson within the nonminimal SUSY model attains a maximum value in the limit of strong Yukawa coupling, in which case  $Y_t(0), Y_\lambda(0) \gg \tilde{\alpha}(0)$ .

From the point of view of a renormalisation group analysis, investigation of the NMSSM presents a much more complicated problem than investigation of the minimal SUSY model. The full set of renormalization group equations within the NMSSM can be found in [30], [34]. Even in the one-loop approximation, this set of equations is nonlinear and its analytic solution does not exist. All equations forming this set can be partitioned into two groups, the first containing equations that describe the evolution of gauge and Yukawa coupling constants. In analysing the nonlinear differential equations entering into this group, it is convenient to go over from  $h_t$ ,  $\lambda$ , and  $\varkappa$  to the quantities  $\rho_t$ ,  $\rho_\lambda$ , and  $\rho_\varkappa$ , which are defined as the ratios of the squares of the corresponding Yukawa coupling constants and the gauge coupling constant for strong interaction,

$$\rho_t(t) = \frac{Y_t(t)}{\tilde{\alpha}_3(t)}, \quad \rho_\lambda(t) = \frac{Y_\lambda(t)}{\tilde{\alpha}_3(t)}, \quad \rho_\varkappa(t) = \frac{Y_\varkappa(t)}{\tilde{\alpha}_3(t)},$$

where  $\tilde{\alpha}_3(t) = g_3^2(t)/(4\pi)^2$ ,  $Y_t(t) = h_t^2(t)/(4\pi)^2$ ,  $Y_\lambda(t) = \lambda^2(t)/(4\pi)^2$ , and  $Y_\varkappa(t) = \varkappa^2(t)/(4\pi)^2$ . The one-loop renormalisation group equations for  $\rho_i(t)$  have the form

$$\begin{aligned} \frac{d\tilde{\alpha}_3}{dt} &= 3\tilde{\alpha}_3^2 \\ \frac{d\rho_1}{dt} &= -\tilde{\alpha}_3\rho_1 \left( \frac{33}{5}\rho_1 + 3 \right) \\ \frac{d\rho_2}{dt} &= -\tilde{\alpha}_3\rho_2 (\rho_2 + 3) \\ \frac{d\rho_t}{dt} &= -\tilde{\alpha}_3\rho_t \left( 6\rho_t + \rho_\lambda - \frac{7}{3} - 3\rho_2 - \frac{13}{15}\rho_1 \right) \\ \frac{d\rho_\lambda}{dt} &= -\tilde{\alpha}_3\rho_\lambda \left( 3\rho_t + 4\rho_\lambda + 2\rho_\varkappa + 3 - 3\rho_2 - \frac{3}{5}\rho_1 \right) \\ \frac{d\rho_\varkappa}{dt} &= -\tilde{\alpha}_3\rho_\varkappa (6\rho_\lambda + 6\rho_\varkappa + 3), \end{aligned} \tag{6}$$

where  $\rho_1(t) = \tilde{\alpha}_1(t)/\tilde{\alpha}_3(t)$ ,  $\rho_2(t) = \tilde{\alpha}_2(t)/\tilde{\alpha}_3(t)$ ,  $\tilde{\alpha}_1(t) = g_1^2(t)/(4\pi)^2$ , and  $\tilde{\alpha}_2(t) = g_2^2(t)/(4\pi)^2$ . The second group includes equations for the parameters of a soft breakdown of SUSY, which are necessary for obtaining a phenomenologically acceptable spectrum of superpartners of observable particles. Since boundary conditions for three Yukawa coupling constants are unknown, it is very difficult to perform a numerical analysis of the equations belonging to the first group and of the full set of the equations given above. In the regime of strong Yukawa coupling, however, solutions to the renormalisation group equations are concentrated in a narrow region of the parameter space near the electroweak scale, and this considerably simplifies the analysis of the set of equations being considered.

### 3 Invariant and quasi–fixed lines; a determination of the quasi–fixed point

Let us first consider the simplest case of  $\varkappa = 0$ . The growth of the Yukawa coupling constant  $\lambda(t_0)$  at a fixed value of  $h_t(t_0)$  results in that the Landau pole in solutions to the renormalization group equations approaches the Grand Unification scale from above. At a specific value  $\lambda(t_0) = \lambda_{\max}$ , perturbation theory at  $q \sim M_X$  cease to be applicable. With increasing (decreasing) Yukawa coupling constant for the  $b$ -quark,  $\lambda_{\max}$  decreases (increases). In the  $(\rho_t, \rho_\lambda)$  plane, the dependence  $\lambda_{\max}^2(h_t^2)$  is represented by a curve bounding the region of admissible values of the parameters  $\rho_t(t_0)$  and  $\rho_\lambda(t_0)$ . At  $\rho_\lambda = 0$ , this curve intersects the abscissa at the point  $\rho_t = \rho_t^{\text{QFP}}(t_0)$ . This is the way in which there arises, in the  $(\rho_t, \rho_\lambda)$  plane, the quasi–fixed (or Hill) line near which solutions to the renormalization group equations for the initial values of the Yukawa coupling constants in the range  $2 \leq h_t^2(0), \lambda^2(0) \leq 10$  are grouped (see Figs. 1a, 1b). With increasing  $\lambda^2(0)$  and  $h_t^2(0)$ , the region where the solutions in questions are concentrated sharply shrinks. At initial values of the Yukawa coupling constants from the range between 20 and 100, they are grouped in a narrow region near the straight line

$$\rho_t(t_0) + 0.506\rho_\lambda(t_0) = 0.91, \quad (7)$$

which can be obtained by fitting the results of numerical calculations (these results are presented in Figs. 2a and 2b). Moreover, it follows from the data in the Table that the combination  $h_t^2(t_0) + 0.506\lambda^2(t_0)$  of the Yukawa coupling constants depends much more weakly on  $\lambda^2(0)$  and  $h_t^2(0)$  than  $\lambda^2(t_0)$  and  $h_t^2(t_0)$  individually. In other words, a decrease in  $\lambda^2(t_0)$  compensates for an increase in  $h_t^2(t_0)$ , and vice versa. To illustrate this, we indicate that, at initial values  $\lambda^2(0)$  and  $h_t^2(0)$  from the interval  $(2, 10)$ , the following occurs upon an increase in  $\lambda^2(0)$  and a decrease in  $h_t^2(0)$ : the constant  $\lambda^2(t_0)$  increases monotonically from 0.191 to 0.421, while  $h_t^2(t_0)$  decreases from 1.199 to 1.051; at the same time, the sum  $h_t^2(t_0) + 0.506\lambda^2(t_0)$  at identical  $\lambda^2(0)$  and  $h_t^2(0)$  ranges between 1.266 and 1.318. The results in Figs. 3a and 3b, which illustrate the evolution of the above combinations of the Yukawa coupling constants, also confirm that this combination is virtually independent of the initial conditions.

In analysing the results of numerical calculations, our attention is engaged by a pronounced nonuniformity in the distribution of solutions to the renormalization group equations along the infrared quasi–fixed line. The main reason for this is that, in the regime of strong Yukawa coupling, the solutions in question are attracted not only to the quasi–fixed but also to the infrared fixed (or invariant) line. The latter connects two fixed points. Of these, one is an infrared fixed point of the set of renormalization group equations within the NMSSM ( $\rho_t = 7/18$ ,  $\rho_\lambda = 0$ ,  $\rho_1 = (\tilde{\alpha}_1/\tilde{\alpha}_3) = 0$ ,  $\rho_2 = (\tilde{\alpha}_2/\tilde{\alpha}_3) = 0$ ) [6], while the other fixed point ( $\rho_\lambda/\rho_t = 1$ ) corresponds to values of the Yukawa coupling constants in the region  $Y_t, Y_\lambda \gg \tilde{\alpha}_i$ , in which case the gauge coupling constants on the right–hand sides of the renormalization group equations can be disregarded [35]. The infrared fixed line is invariant under renormalization group transformations – that is, it is independent of the scale at which the boundary values  $Y_t(0)$  and  $Y_\lambda(0)$  are specified and of the boundary values themselves. If the boundary conditions are such that  $Y_t(0)$  and  $Y_\lambda(0)$  belong to the fixed line, the evolution of the Yukawa coupling constants proceeds further along this line toward the infrared fixed point of the set of renormalization

group equations within the NMSSM. With increasing  $t$ , all other solutions to the renormalization group equations are attracted to the infrared fixed line and, for  $t/(4\pi) \gg 1$ , approach the stable infrared fixed point. From the data in Figs. 1b and 2b, it follows that, with increasing  $Y_t(0)$  and  $Y_\lambda(0)$ , all solutions to the renormalization group equations are concentrated in the vicinity of the point of intersection of the infrared fixed and the quasi-fixed line:

$$\rho_t^{\text{QFP}}(t_0) = 0.803, \quad \rho_\lambda^{\text{QFP}}(t_0) = 0.224.$$

Hence, this point can be considered as the quasi-fixed point of the set of renormalization group equations within the NMSSM at  $\varkappa = 0$ .

Infrared fixed lines and surfaces, as well as their properties in the minimal Standard Model and in the minimal SUSY model, were studied in detail in [7], [20], [36]. Within the NMSSM, the emergence of fixed lines can be traced at  $\lambda = 0$ , in which case the set of renormalization group equations for the Yukawa coupling constants reduced to two independent differential equations – of these, one coincides with the equation for  $Y_t(t)$  in the minimal SUSY model, while the other describes the evolution of  $Y_\varkappa(t)$ . In the limit being considered, the set of one-loop renormalization group equations has the exact analytic solution

$$\begin{aligned} Y_\varkappa(t) &= \frac{Y_\varkappa(0)}{1 + 6Y_\varkappa(0)t}, \\ Y_t(t) &= \frac{Y_t(0)E(t)}{1 + 6Y_t(0)F(t)}, \\ \tilde{\alpha}_i(t) &= \frac{\tilde{\alpha}_i(0)}{1 + b_i\alpha_i(0)t}, \end{aligned} \tag{8}$$

where the expressions for  $E(t)$ ,  $F(t)$ , and  $b_i$  are presented in the Appendix. The quasi-fixed line in the  $(\rho_t, \rho_\varkappa)$  plane includes two straight lines parallel to the coordinate axes (see Fig. 4b),

$$\begin{aligned} \rho_t &= \frac{E(t_0)}{6\tilde{\alpha}_3(t_0)F(t_0)} \approx 0.876, \\ \rho_\varkappa &= \frac{1}{6\tilde{\alpha}_3(t_0)t_0} \approx 0.280, \end{aligned} \tag{9}$$

which intersects at the point  $(0.876, 0.280)$ . Since the above solutions to the renormalization group equations are attracted to the invariant line at  $t/(4\pi) \gg 1$ , unity can be disregarded in the denominators of  $Y_t(t)$  and  $Y_\varkappa(t)$ . The infrared fixed line can then be specified parametrically:

$$\begin{aligned} \rho_t(t) &= \frac{E(t)}{6\tilde{\alpha}_3(t)F(t)} \\ \rho_\varkappa(t) &= \frac{1}{6\tilde{\alpha}_3(t)t}. \end{aligned} \tag{10}$$

It can easily be shown that the limit  $t \rightarrow 0$  corresponds to the values  $\rho_t$  and  $\rho_\varkappa \gg 1$  belonging to this curve,  $\rho_t$  and  $\rho_\varkappa$  being virtually coincident in this limit.



By using the expansions of the functions  $E(t)$  and  $F(t)$  in the vicinity of the origin,  $F(t) \approx t + 0.5E'(0)t^2 + \dots$  and  $E(t) \approx 1 + E'(0)t + \dots$ , we obtain

$$\rho_{\varkappa} = \rho_t - \frac{4}{9} - \frac{\rho_2}{4} - \frac{13}{180}\rho_1. \quad (11)$$

The equality  $\rho_{\varkappa} = \rho_t$  corresponds to the stable fixed point of the renormalization group equations in the regime of strong Yukawa coupling ( $\rho_{\varkappa}, \rho_t \gg 1$ ). As  $\tilde{\alpha}_3$  tends to the Landau pole for  $t \rightarrow t_c = 1/(3\tilde{\alpha}_3(0))$ , however, the line given by Eq.(10) approaches the stable infrared point (see Fig. 4b); that is,  $\rho_t(t)$  tends to  $7/18$ , while  $\rho_{\varkappa}(t)$  vanishes:  $\rho_{\varkappa} \sim (\rho_t - 7/18)^{9/7}$ . The curve given by (10), which connects the fixed points  $\rho_{\varkappa}/\rho_t = 1$  and  $\rho_{\varkappa} = 0$ ,  $\rho_t = 7/18$  intersects the quasi-fixed line at the point  $(0.876, 0.280)$ . As can be seen from Fig. 4b, solutions to the renormalization group equations are concentrated precisely in the vicinity of this point.

Near the infrared fixed point, the curve being investigated is tangent to another invariant line, that which is specified by the equation  $\rho_{\varkappa} = 0$ . This line connects the unstable fixed point  $\rho_{\varkappa}/\rho_t = 0$ , which arises in the regime of strong Yukawa coupling ( $\rho_t \gg 1$ ), with other fixed points, those at  $\rho_{\varkappa} = 0$ ,  $\rho_t = 7/18$  and at  $\rho_{\varkappa} = \rho_t = 0$ , the last also being unstable. Yet another infrared fixed line – the attraction of solutions to the renormalization group equations to this line as the weakest – passes through the points  $\rho_t/\rho_{\varkappa} = 0$  and  $\rho_t = 7/18$ ,  $\rho_{\varkappa} = 0$ . At  $\tilde{\alpha}_1 = \tilde{\alpha}_2 = 0$ , it appears to be a straight line parallel to the coordinate axis,  $\rho_t = 7/18$ . However, the inclusion of electroweak interactions leads to a monotonic decrease in  $\rho_t(t)$  with increasing  $\rho_{\varkappa}(t)$ . In the vicinity of the stable infrared fixed point for  $t \rightarrow t_c$ , the equation for this line has the form

$$\begin{aligned} \rho_t(t) &= \frac{7}{18} - \frac{7}{4}\rho_2(t) - \frac{91}{180}\rho_1(t) \\ \rho_{\varkappa}(t) &= \frac{1}{6\tilde{\alpha}_3(t)t}. \end{aligned} \quad (12)$$

Apart from the replacement of  $\rho_{\varkappa}$  by  $\rho_{\lambda}$ , the same infrared fixed lines are involved in the analysis of renormalization group equations within the NMSSM in the case where  $\varkappa = 0$ . As before, the invariant line that connects the stable fixed points  $\rho_{\lambda}/\rho_t = 1$  and  $\rho_t = 7/18$ ,  $\rho_{\lambda} = 0$  attracts most strongly solutions to the renormalization group equations. Nevertheless, the asymptotic behaviour of the curve being studied changes for  $\rho_{\lambda}, \rho_t \gg 1$ , where it becomes

$$\rho_{\lambda} = \rho_t - \frac{8}{15} - \frac{2}{75}\rho_1, \quad (13)$$

and in the vicinity of the point  $\rho_t = 7/18$ ,  $\rho_{\lambda} = 0$ , where we have  $\rho_{\lambda} \sim (\rho_t - 7/18)^{25/14}$ . In analysing the behaviour of solutions to the renormalization group equations, the other two invariant lines have but a marginal effect. One of these is specified by the equations  $\rho_{\lambda} = 0$ . The second connects the unstable fixed point in the regime of strong Yukawa coupling,  $\rho_t/\rho_{\lambda} = 0$ , with the stable infrared point, near which we have  $\rho_{\lambda} \sim (7/18 - \rho_t)^{25/18}$ .

## 4 Invariant and Hill surfaces

In a more complicated case where all three Yukawa coupling constants in the NMSSM are nonzero, analysis of the set of renormalization group equations presents a much more

difficult problem. In particular, invariant (infrared fixed) and Hill surfaces come to the fore instead of the infrared fixed and quasi-fixed lines. For each fixed set of values of the coupling constants  $Y_t(t_0)$  and  $Y_{\mathcal{Z}}(t_0)$ , an upper limit on  $Y_\lambda(t_0)$  can be obtained from the requirement that perturbation theory be applicable up to the Grand Unification scale  $M_X$ . A change in the values of the Yukawa coupling constants  $h_t$  and  $\mathcal{Z}$  at the electroweak scale leads to a growth or a reduction of the upper limit on  $Y_\lambda(t_0)$ . The resulting surface in the  $(\rho_t, \rho_{\mathcal{Z}}, \rho_\lambda)$  space is shown in Figs. 5a and 5b. In the regime of strong Yukawa coupling, solutions to the renormalization group equations are concentrated near this surface. In just the same way as in the case of  $Y_{\mathcal{Z}} = 0$ , a specific linear combination of  $Y_t$ ,  $Y_\lambda$ , and  $Y_{\mathcal{Z}}$  is virtually independent of the initial conditions for  $Y_i(0) \rightarrow \infty$ :

$$\rho_t(t_0) + 0.72\rho_\lambda(t_0) + 0.33\rho_{\mathcal{Z}}(t_0) = 0.98. \quad (14)$$

For  $2 \leq h_t^2(0), \mathcal{Z}^2(0), \lambda^2(0) \leq 10$ , this combination of the coupling constants,  $h_t^2(t_0) + 0.72\lambda^2(t_0) + 0.33\mathcal{Z}^2(t_0)$ , ranges between 1.35 and 1.40; at the same time, we have  $1.058 \leq h_t^2(t_0) \leq 1.219$ ,  $0.032 \leq \mathcal{Z}^2(t_0) \leq 0.296$ ,  $0.098 \leq \lambda^2(t_0) \leq 0.401$  (see Table). The evolution of  $\rho_t(t) + 0.72\rho_\lambda(t) + 0.33\rho_{\mathcal{Z}}(t)$  at various initial values of the Yukawa coupling constants is illustrated in Fig. 6.

On the Hill surface, the region that is depicted in Fig. 5 and near which the solutions in question are grouped shrinks in one direction with increasing initial values of the Yukawa coupling constants, with the result that, at  $Y_t(0)$ ,  $Y_{\mathcal{Z}}(0)$ , and  $Y_\lambda(0) \sim 1$ , all solutions are grouped around the line that appears as the result of intersection of the quasi-fixed surface and the infrared fixed surface, which includes the invariant lines lying in the  $\rho_{\mathcal{Z}} = 0$  and  $\rho_\lambda = 0$  planes and connecting the stable infrared point with, respectively, the fixed point  $\rho_\lambda/\rho_t = 1$  and the fixed point  $\rho_{\mathcal{Z}}/\rho_t = 1$  in the regime of strong Yukawa coupling. In the limit  $\rho_t, \rho_\lambda, \rho_{\mathcal{Z}} \gg 1$ , in which case the gauge coupling constants can be disregarded, the fixed points  $\rho_\lambda/\rho_t = 1$ ,  $\rho_{\mathcal{Z}}/\rho_t = 0$  and  $\rho_{\mathcal{Z}}\rho_t = 1$ ,  $\rho_\lambda/\rho_t = 0$  cease to be stable. Instead of them, the stable fixed point  $R_\lambda = 3/4$ ,  $R_{\mathcal{Z}} = 3/8$  [35] appears in the  $(R_\lambda, R_{\mathcal{Z}})$  plane, where  $R_\lambda = \rho_\lambda/\rho_t$  and  $R_{\mathcal{Z}} = \rho_{\mathcal{Z}}/\rho_t$ . In order to investigate the behaviour of the solutions to the renormalization group equations within the NMSSM, it is necessary to linearise the set of these equations in its vicinity and set  $\alpha_i = 0$ . As a result, we obtain

$$\begin{aligned} R_\lambda(t) &= \frac{3}{4} + \left( \frac{1}{2}R_{\lambda 0} + \frac{1}{\sqrt{5}}R_{\mathcal{Z}0} - \frac{3(\sqrt{5}+1)}{8\sqrt{5}} \right) \left( \frac{\rho_t(t)}{\rho_{t0}} \right)^{\lambda_1} \\ &\quad + \left( \frac{1}{2}R_{\lambda 0} - \frac{1}{\sqrt{5}}R_{\mathcal{Z}0} - \frac{3(\sqrt{5}-1)}{8\sqrt{5}} \right) \left( \frac{\rho_t(t)}{\rho_{t0}} \right)^{\lambda_2}, \\ R_{\mathcal{Z}}(t) &= \frac{3}{8} + \frac{\sqrt{5}}{2} \left( \frac{1}{2}R_{\lambda 0} + \frac{1}{\sqrt{5}}R_{\mathcal{Z}0} - \frac{3(\sqrt{5}+1)}{8\sqrt{5}} \right) \left( \frac{\rho_t(t)}{\rho_{t0}} \right)^{\lambda_1} \\ &\quad - \frac{\sqrt{5}}{2} \left( \frac{1}{2}R_{\lambda 0} - \frac{1}{\sqrt{5}}R_{\mathcal{Z}0} - \frac{3(\sqrt{5}-1)}{8\sqrt{5}} \right) \left( \frac{\rho_t(t)}{\rho_{t0}} \right)^{\lambda_2}, \end{aligned} \quad (15)$$

where  $R_{\lambda 0} = R_\lambda(0)$ ,  $R_{\mathcal{Z}0} = R_{\mathcal{Z}}(0)$ ,  $\rho_{t0} = \rho_t(0)$ ,  $\lambda_1 = \frac{3+\sqrt{5}}{9}$ ,  $\lambda_2 = \frac{3-\sqrt{5}}{9}$ , and  $\rho_t(t) = \frac{\rho_{t0}}{1+7\rho_{t0}t}$ . From (15), it follows that the fixed point  $R_\lambda = 3/4$ ,  $R_{\mathcal{Z}} = 3/8$  arises as the result of intersection of two fixed lines in the  $(R_\lambda, R_{\mathcal{Z}})$  plane. The solutions

are attracted most strongly to the line  $\frac{1}{2}R_\lambda + \frac{1}{\sqrt{5}}R_\varkappa = \frac{3}{8}\left(1 + \frac{1}{\sqrt{5}}\right)$ , since  $\lambda_1 \gg \lambda_2$ .

This line passes through three fixed points in the  $(R_\lambda, R_\varkappa)$  plane:  $(1, 0)$ ,  $(3/4, 3/8)$ , and  $(0, 1)$ . In the regime of strong Yukawa coupling, the fixed line that corresponds, in the  $(\rho_t, \rho_\varkappa, \rho_\lambda)$  space, to the line mentioned immediately above is that which lies on the invariant surface containing a stable infrared fixed point. The line of intersection of the Hill and the invariant surface can be obtained by mapping this fixed line into the quasi-fixed surface with the aid of the set of renormalization group equations. For the boundary conditions, one must than use the values  $\lambda^2(0)$ ,  $\varkappa^2(0)$ , and  $h_t^2(0) \gg 1$  belonging to the aforementioned fixed line.

In just the same way as infrared fixed lines, the infrared fixed surface is invariant under renormalization group transformations. In the evolution process, solutions to the set of renormalization group equations within the NMSSM are attracted to this surface. If boundary conditions are specified n the fixed surface, the ensuing evolution of the coupling constants proceeds within this surface. To add further details, we not that, near the surface being studied and on it, the solutions are attracted to the invariant line connecting the stable fixed point  $(\rho_\lambda/\rho_t = 3/4, \rho_\varkappa/\rho_t = 3/8)$  in the regime of strong Yukawa coupling with the stable infrared fixed point within the NMSSM. In the limit  $\rho_t, \rho_\varkappa, \rho_\lambda \gg 1$ , the equation for this line has the form

$$\begin{aligned}\rho_\lambda &= \frac{3}{4}\rho_t - \frac{176}{417} + \frac{3}{139}\rho_2 - \frac{7}{417}\rho_1, \\ \rho_\varkappa &= \frac{3}{8}\rho_t - \frac{56}{417} - \frac{18}{139}\rho_2 - \frac{68}{2085}\rho_1.\end{aligned}\tag{16}$$

As one approaches the infrared fixed point, the quantities  $\rho_\lambda$  and  $\rho_\varkappa$  tend to zero:  $\rho_\lambda \sim (\rho_t - 7/18)^{25/14}$  and  $\rho_\varkappa \sim (\rho_t - 7/18)^{9/7}$ . This line intersects the quasi-fixed surface at the point

$$\rho_t^{\text{QFP}}(t_0) = 0.82, \quad \rho_\varkappa^{\text{QFP}}(t_0) = 0.087, \quad \rho_\lambda^{\text{QFP}}(t_0) = 0.178.$$

Since all solutions are concentrated in the vicinity of this point for  $Y_t(0), Y_\lambda(0), Y_\varkappa(0) \rightarrow \infty$ , it should be considered as a quasi-fixed point for the set of renormalization group equations within the NMSSM. We note, however, that the solutions are attracted to the invariant line (16) and to the quasi-fixed line on the Hill surface. This conclusion can be drawn from the an analysis of the behaviour of the solutions near the fixed point  $(R_\lambda = 3/4, R_\varkappa = 3/8)$  (see Eq.(15)). Once the solutions have approached the invariant line  $\frac{1}{2}R_\lambda + \frac{1}{\sqrt{5}}R_\varkappa = \frac{3}{8}\left(1 + \frac{1}{\sqrt{5}}\right)$ , their evolution is governed by the expression  $(\epsilon(t))^{0.085}$ , where  $\epsilon(t) = \rho_t(t)/\rho_{t0}$ . This means that the solutions begin to be attracted to the quasi-fixed point and to the invariant line (16) with a sizable strength only when  $Y_i(0)$  reaches a value of  $10^2$ , at which perturbation theory is obviously inapplicable. Thus, it is not the infrared quasi-fixed point but the quasi-fixed line on the Hill surface (see Fig. 5) that, within the NMSSM, plays a key role in analysing the behaviour of the solutions to the renormalization group equations in the regime of strong Yukawa coupling, where all  $Y_i(0)$  are much greater than  $\tilde{\alpha}(0)$ .

Along with the invariant surface, which was studied in detail above, at least three infrared fixed surfaces exist in the  $(\rho_t, \rho_\varkappa, \rho_\lambda)$  space. They attract solutions to the renormalization group equations much more weakly. Two of these are specified by the equations  $\rho_\lambda$  and

$\rho_\varkappa = 0$ . Yet another infrared fixed surface can be found by analysing the behaviour of the solutions in question near the stable infrared fixed point. Integrating the linearised renormalisation group equations, we obtain

$$\begin{aligned}
\rho_t(t) &= \frac{7}{18} + \left( \rho'_{t0} - \frac{7}{33}\rho_{\lambda 0} + \frac{7}{4}\rho_{20} + \frac{91}{180}\rho_{10} - \frac{7}{18} \right) \left( \frac{\tilde{\alpha}_{30}}{\tilde{\alpha}_3(t)} \right)^{7/9} \\
&\quad + \frac{7}{33}\rho_\lambda(t) - \frac{7}{4}\rho_2(t) - \frac{91}{180}\rho_1(t), \\
\rho_\lambda(t) &= \rho_{\lambda 0} \left( \frac{\tilde{\alpha}_{30}}{\tilde{\alpha}_3(t)} \right)^{25/18}, \\
\rho_\varkappa(t) &= \rho_{\varkappa 0} \left( \frac{\tilde{\alpha}_{30}}{\tilde{\alpha}_3(t)} \right),
\end{aligned} \tag{17}$$

where  $\rho'_{t0}$ ,  $\rho_{i0}$ , and  $\tilde{\alpha}_{30}$  are constants of integration. In the limiting case of  $\rho_1 = \rho_2 = 0$ , the equation of a nontrivial invariant surface is  $\rho_t = \frac{7}{18} + \frac{7}{33}\rho_\lambda$ . This surface contains nontrivial infrared fixed lines that lie in the  $\rho_\lambda = 0$  and  $\rho_\varkappa = 0$  planes and which weakly attract solutions to the renormalization group equations. The inclusion of electroweak interactions significantly modifies the asymptotic behaviour of this surface near the infrared fixed point. Nonetheless, a solution to the linearised equations (17) does not fix unambiguously an equations for this surface. Considering that, at  $\rho_\lambda = 0$ , the equation of the surface being studied must reduce to the equation for the invariant line (12), we find, for  $t \rightarrow t_c$ , that

$$\rho_t = \frac{7}{18} + \frac{7}{33}\rho_\lambda - 6t_c \left( \frac{7}{4}\tilde{\alpha}_2(t_c) + \frac{91}{180}\tilde{\alpha}_1(t_c) \right) \rho_\varkappa. \tag{18}$$

Relation (18) between  $\rho_t$ ,  $\rho_\lambda$ , and  $\rho_\varkappa$  is valid for  $\rho_\varkappa \gg \rho_\lambda$ . By analysing the behaviour of the solutions in the vicinity of the stable infrared point (17), it can be shown that the invariant surface (18) plays a secondary role in the NMSSM.

## 5 Approximate solutions for the Yukawa couplings

By way of example, the emergence of quasi-fixed lines and surfaces within the NMSSM can be traced by considering approximate solutions to the renormalisation group equations from the Appendix. Recently, approximate solutions of this type were studied within the minimal SUSY model for  $\tan \beta \gg 1$  [37], in which case  $Y_t \sim Y_b \sim Y_\tau$ . In the regime of strong Yukawa coupling within the nonminimal SUSY model, these solutions are given by

$$\begin{aligned}
\rho_t(t) &= \frac{E_t(t)}{\tilde{\alpha}_3(t) [6F_t(t)(6F_t(t) + 2R_{\lambda 0}F_\lambda(t))]^{1/2}} + O\left(\frac{1}{Y_t(0)}\right) + \dots, \\
\rho_\lambda(t) &= \frac{R_{\lambda 0}E_\lambda(t)}{\tilde{\alpha}_3(t) (6R_{\lambda 0}F_\lambda(t) + 6R_{\varkappa 0}t)^{1/3} (6R_{\lambda 0}F_\lambda(t))^{1/6} (6F_t(t) + 2R_{\lambda 0}F_\lambda(t))^{1/2}} \\
&\quad + O\left(\frac{1}{Y_t(0)}\right) + \dots, \\
\rho_\varkappa(t) &= \frac{R_{\varkappa 0}}{\tilde{\alpha}_3(t) (6R_{\lambda 0}F_\lambda(t) + 6R_{\varkappa 0}t)} + O\left(\frac{1}{Y_t(0)}\right) + \dots,
\end{aligned} \tag{19}$$

where the expressions for the functions  $E_i(t)$  and  $F_i(t)$  are presented in the Appendix. Expressions (19) for  $\rho_i(t)$  were formally obtained by expanding approximate solutions in a power series in  $1/Y_t(0)$ . Each subsequent term in such an expansion is always much less than the preceding one because, in the approximate solutions, the Yukawa coupling constant for the  $t$ -quark always appears in the form of the combination  $Y_t(0)F_t(t)$ , which, in the regime of strong Yukawa coupling, leads to values  $\frac{1}{Y_t(0)F_t(t)} \ll 1$  at  $t \sim t_0$ . From relations (19), it follows that, to  $O(1/Y_t(0))$  terms, solutions to the renormalisation group equations depend only on the ratios of the Yukawa coupling constants  $R_{\lambda 0}$  and  $R_{\varkappa 0}$  at the Grand Unification scale. Setting  $t = t_0$ , we obtain a surface in the  $(\rho_t, \rho_{\varkappa}, \rho_\lambda)$  space. This surface is specified parametrically; that is,  $\rho_i = G_i(R_{\lambda 0}, R_{\varkappa 0})$ . Deviations from it are determined by  $O(1/Y_t(0))$  terms, which are negative and small in magnitude in the limit of strong Yukawa coupling.

However, the approximate solutions (19) poorly describe the evolution of  $\rho_{\varkappa}(t)$ . By way of example, we indicate that, at the electroweak scale, the relative error is about 20% at  $\varkappa^2(t_0) \sim 0.1$ . This is due above all to the fact that the self-interaction constant for the scalar field  $Y$  is not renormalised by gauge interactions. The greater the contribution of gauge interactions to the renormalisation of Yukawa coupling constants, the higher the accuracy to which the approximate solutions describe their evolution. For example, the relative error in  $\rho_t(t_0)$  ( $\rho_\lambda(t_0)$ ) is 2 – 3% (about 5 – 6%) at  $Y_t(0) \sim Y_{\varkappa}(0) \sim Y_\lambda(0)$ .

An approximate solution for  $Y_{\varkappa} = 0$  and  $Y_t(0), Y_\lambda(0) \gg \tilde{\alpha}_i(0)$  can be obtained by setting  $R_{\varkappa 0} = 0$  in Eqs.(19). In the regime of strong Yukawa coupling,  $\rho_t(t)$  and  $\rho_\lambda(t)$  then depend only on  $R_{\lambda 0}$ , with the result that, in the  $(\rho_t, \rho_\lambda)$  plane, there arises, at  $t = t_0$ , the Hill line

$$\rho_t^2 + \frac{1}{3} \left( \frac{E_t(t_0)}{E_\lambda(t_0)} \right)^2 \left( \frac{F_\lambda(t_0)}{F_t(t_0)} \right)^2 \rho_\lambda^2 = \rho_{\text{QFP}}^2, \quad (20)$$

where  $\rho_{\text{QFP}} = \frac{E_t(t_0)}{6F_t(t_0)\alpha_3(t_0)}$ . With increasing initial values of the Yukawa coupling constants,  $O(1/Y_t(0))$  terms, which determine the deviation of the solutions in question from the quasi-fixed line (20), decrease, so that the approximate solutions to the renormalisation group equations within the NMSSM are attracted to this line. The explicit form of the dependences  $\rho_\lambda(t)$  and  $\rho_t(t)$  in (19) makes it possible to find that the invariant line lying in the  $(\rho_t, \rho_\lambda)$  plane and corresponding to  $R_{\lambda 0} = 1$  can be approximately parametrised as

$$\begin{aligned} \rho_t(t) &= \frac{E_t(t)}{\tilde{\alpha}_3(t) [6F_t(t)(6F_t(t) + 2F_\lambda(t))]^{1/2}} \\ \rho_\lambda(t) &= \frac{E_\lambda(t)}{\tilde{\alpha}_3(t) [6F_\lambda(t)(6F_t(t) + 2F_\lambda(t))]^{1/2}}. \end{aligned} \quad (21)$$

The values  $\rho_t(t_0)$  and  $\rho_\lambda(t_0)$  as calculated by formulas (21) are the coordinates of the point where the Hill fixed line (20) intersects the infrared fixed line (21), which appears to be a quasi-fixed point for the set of renormalisation group equations within the NMSSM. Our numerical results, which are displayed in Fig. 7, demonstrate that relations (20) and (21) reproduce quite accurately the quasi-fixed and the invariant line at  $R_{\lambda 0} \leq 1$ . Significant deviations are observed only in the infrared region ( $t \rightarrow t_c$ ) and for  $R_{\lambda 0} \gg 1$ . In general, the relative deviation of the approximate solution in question from the exact one is 5 – 6% at  $\rho_{\varkappa} = 0$  and  $R_{\lambda 0} \sim 1$  and grows fast with increasing  $\rho_\lambda/\rho_t$ .

## 6 Unification of the Yukawa couplings $h_b$ and $h_\tau$

As was indicated above, Grand Unification Theory imposes additional constraints on the parameter space of SUSY models. Among such constraints, the unification of the Yukawa coupling constants for the  $b$ -quark and the  $\tau$ -lepton at the scale  $M_X$  is worthy of note above all. In the nonminimal SUSY model,  $h_b$  and  $h_\tau$  are unified if the constants  $Y_t$ ,  $Y_\lambda$ , and  $Y_\varkappa$  satisfy the relations:

$$\begin{aligned} \frac{Y_t(0)}{Y_t(t_0)} &= \left[ \frac{R_{b\tau}(0)}{R_{b\tau}(t_0)} \right]^{\frac{21}{2}} \left[ \frac{\tilde{\alpha}_3(t_0)}{\tilde{\alpha}_3(0)} \right]^{\frac{68}{9}} \left[ \frac{\tilde{\alpha}_2(t_0)}{\tilde{\alpha}_2(0)} \right]^{\frac{9}{4}} \left[ \frac{\tilde{\alpha}_1(t_0)}{\tilde{\alpha}_1(0)} \right]^{\frac{463}{396}} \left[ \frac{Y_\lambda(0)}{Y_\lambda(t_0)} \right]^{\frac{1}{4}}, \\ \frac{Y_t(0)}{Y_t(t_0)} &= \left[ \frac{R_{b\tau}(0)}{R_{b\tau}(t_0)} \right]^9 \left[ \frac{\tilde{\alpha}_3(t_0)}{\tilde{\alpha}_3(0)} \right]^{\frac{56}{9}} \left[ \frac{\tilde{\alpha}_2(t_0)}{\tilde{\alpha}_2(0)} \right]^{\frac{3}{2}} \left[ \frac{\tilde{\alpha}_1(t_0)}{\tilde{\alpha}_1(0)} \right]^{\frac{197}{198}} \left[ \frac{Y_\lambda(0)}{Y_\lambda(t_0)} \right]^{\frac{1}{2}} \left[ \frac{Y_\varkappa(t_0)}{Y_\varkappa(0)} \right]^{\frac{1}{6}}, \end{aligned} \quad (22)$$

where  $R_{b\tau}(t_0) = m_b(t_0)/m_\tau(t_0)$  is the ratio of the running masses of the  $b$ -quark and the  $\tau$ -lepton at the electroweak scale; in the minimal unification schemes we have

$R_{b\tau}(0) = \sqrt{\frac{Y_b(0)}{Y_\tau(0)}} = 1$ . The equation determining the function  $R_{b\tau}(t)$  is presented in the Appendix (see Eq.(25)). The first relation in (22) corresponds to the case of  $\varkappa = 0$ , whereas the second implies a  $\varkappa$  value different from zero. Relations (22) can be obtained by directly integrating the renormalisation group equations. Setting  $R_{b\tau}(t_0) = 1.61$ , which corresponds to  $m_b(t_0) = 2.86$  GeV and  $m_\tau(t_0) = 1.78$  GeV, we find, for the ratio of the Yukawa coupling constants for the  $t$ -quark, that

$$\frac{Y_t(0)}{Y_t(t_0)} \approx 3.67 \left[ \frac{Y_\lambda(0)}{Y_\lambda(t_0)} \right]^{1/4}, \quad \frac{Y_t(0)}{Y_t(t_0)} \approx 2.57 \left[ \frac{Y_\lambda(0)}{Y_\lambda(t_0)} \right]^{1/2} \left[ \frac{Y_\varkappa(t_0)}{Y_\varkappa(0)} \right]^{1/6}. \quad (23)$$

The second equation in (23) – it relates  $Y_t$ ,  $Y_\lambda$ , and  $Y_\varkappa$  – determines a surface in the  $(\rho_t, \rho_\lambda, \rho_\varkappa)$  space; at  $Y_\varkappa = 0$ , this surface degenerates into a line in the  $(\rho_t, \rho_\lambda)$  plane. In this case,  $b - \tau$  unification is possible under the condition  $Y_t(0) \gg Y_t(t_0)$ , which is realised only in the regime of strong Yukawa coupling within the NMSSM. In the  $(\rho_t, \rho_\lambda)$  plane, Fig. 8 shows the Hill line and the curve that corresponds to  $Y_b(0) = Y_\tau(0)$ . As might have been expected, the spacing between them is quite small. In addition, we note that only at sufficiently large values of the  $t$ -quark Yukawa coupling constant at the electroweak scale,  $Y_t(t_0) > Y_t^0$ , is  $b - \tau$  unification possible. A lower limit on the  $Y_t(t_0)$  implies that there exists an upper limit on  $\tan\beta$  (see Eq.(1)). By varying the running  $b$ -quark mass  $m_b(m_b)$  from 4.1 to 4.4 GeV, we found that only for  $\tan\beta \leq 2$  can the equality of the Yukawa coupling constants at the Grand Unification scale be achieved. The possibility of unifying the Yukawa coupling constants within the NMSSM was investigated in detail elsewhere [38]. The condition  $Y_b(0) = Y_\tau(0)$  imposes stringent constraints on the parameter space of the model being studied. Since  $h_b$  and  $h_\tau$  are small in magnitude at  $\tan\beta \sim 1$ , they can be generated, however, at the Grand Unification scale owing to unrenormalised operators upon a spontaneous breakdown of symmetry, in which case  $h_b$  and  $h_\tau$  can take different values.

## 7 Conclusion

The present analysis has revealed that, in the regime of strong Yukawa coupling, solutions to the renormalisation group equations within the NMSSM,  $Y_i(t)$ , are attracted to quasi-fixed lines and surfaces in the space of Yukawa coupling constants and that specific combinations  $\rho_i(t)$  are virtually independent of their initial values at the Grand Unification scale. It is for  $Y_i(0) \gg \tilde{\alpha}_i(0)$  that the upper limit on the mass of the lightest Higgs boson attains its maximum value. It has also been proven that, in the limit being considered, the values of the constants  $h_t$ ,  $\lambda$ , and  $\varkappa$  can be chosen in such a way as to ensure unification of the Yukawa coupling constants for the  $b$ -quark and  $\tau$ -lepton at the scale  $M_X$ , a feature usually inherent in Grand Unified Theories. For  $Y_i(0) \rightarrow \infty$ , all solution to the renormalisation group equations are concentrated near quasi-fixed points. These points emerge as the result of intersection of Hill lines or surfaces with the invariant line that connects the stable fixed point for  $Y_i \gg \tilde{\alpha}_i$  with the stable infrared fixed point. For the renormalisation group equations within the NMSSM, we have listed all the most important invariant lines and surfaces and studied their asymptotic behaviour for  $Y_i \gg \tilde{\alpha}_i$  and in the vicinity of the infrared fixed point.

With increasing  $Y_i(0)$ , the solutions in question approach quasi-fixed points quite slowly; that is, the deviation is proportional to  $(\epsilon_t(t))^\delta$ , where  $\epsilon_t(t) = Y_t(t)/Y_t(0)$  and  $\delta$  is calculated by analysing the set of the renormalisation group equations in the regime of strong Yukawa coupling. As a rule,  $\delta$  is positive and much less than unity. By way of example, we indicate that, in the case where all three Yukawa coupling constants differ from zero,  $\delta \approx 0.085$ . Of greatest importance in analysing the behaviour of solutions to the renormalisation group equations within the NMSSM at  $Y_t(0), Y_\lambda(0), Y_\varkappa(0) \sim 1$  is therefore not the infrared quasi-fixed point but the line lying on the Hill surface and emerging as the intersection of the Hill and invariant surface. This line can be obtained by mapping the fixed points  $(1, 0)$ ,  $(3/4, 3/8)$ , and  $(0, 1)$  in the  $(R_\lambda, R_\varkappa)$  plane for  $Y_i \gg \tilde{\alpha}_i$  into the quasi-fixed surface by means of renormalisation group equations.

The emergence of Hill lines and surfaces in the space of Yukawa coupling constants can be traced by considering the examples of approximate solutions that are presented in the Appendix. These solutions lead to qualitatively correct results. However, the approximate solutions poorly describe the evolution of  $Y_\varkappa(t)$ , since the neutral field  $Y$  is not renormalised by gauge interactions. At the same time, it has been shown that, at  $Y_t(0) \sim Y_\lambda(0)$ , the relative deviation of the approximate solution from the exact one is as small as 2–3% in  $Y_t(t_0)$  and about 5–6% in  $Y_\lambda(t_0)$ . With increasing  $Y_\lambda(t_0)/Y_t(t_0)$ , such relative deviations grow quite fast.

## Acknowledgements

The authors are grateful to M.I.Vysotsky, D.I.Kazakov, and K.A.Ter-Martirosyan for stimulating questions, valuable discussions, and enlightening comments. R.B.Nevzorov is indebted to Instituto Nazionale di Fisica Nucleare (Sezione di Ferrara) for the kind hospitality extended to him.

This work was supported by the Russian Foundation for Basic Research (RFBR), projects ## 98-02-17372, 98-02-17453, 96-15-96578, 96-15-96740; by INTAS, project # 93-3316-

Ext.; by a joint RFBR–INTAS grant # 95-0567.



# Appendix

## Set of the renormalisation group equations of the NMSSM for the Yukawa couplings and an approximate solution to it.

In the present study we have analysed the one-loop renormalisation group equations within the NMSSM. These equations can be represented as [34]:

$$\begin{aligned}
\frac{d\tilde{\alpha}_i}{dt} &= -b_i\tilde{\alpha}_i^2, \\
\frac{dY_t}{dt} &= -Y_t(Y_\lambda + 6Y_t - \frac{16}{3}\tilde{\alpha}_3 - 3\tilde{\alpha}_2 - \frac{13}{15}\tilde{\alpha}_1), \\
\frac{dY_\lambda}{dt} &= -Y_\lambda(4Y_\lambda + 2Y_\varkappa + 3Y_t - 3\tilde{\alpha}_2 - \frac{3}{5}\tilde{\alpha}_1), \\
\frac{dY_\varkappa}{dt} &= -6Y_\varkappa(Y_\lambda + Y_\varkappa).
\end{aligned}
\tag{24}$$

On the right-hand sides of these differential equations we have discarded terms proportional to the Yukawa couplings  $Y_b$  and  $Y_\tau$ , since their contribution at  $\tan\beta \ll 10$  is negligibly small. The index  $i$  runs through the values from 1 and 3,  $b_1 = \frac{33}{5}$ ,  $b_2 = 1$ ,  $b_3 = -3$ ,  $\tilde{\alpha}_i(t) = \frac{\alpha_i(t)}{4\pi} = \left(\frac{g_i(t)}{4\pi}\right)^2$ ,  $Y_t(t) = \left(\frac{h_t(t)}{4\pi}\right)^2$ ,  $Y_\lambda(t) = \left(\frac{\lambda(t)}{4\pi}\right)^2$ , and  $Y_\varkappa(t) = \left(\frac{\varkappa(t)}{4\pi}\right)^2$ . The variable  $t$  is defined in a standard way:  $t = \ln\left(\frac{M_X^2}{Q^2}\right)$ , where  $M_X = 3 \cdot 10^{16}$  GeV.

In analysing  $b - \tau$  unification, use was made of the evolution equation for the ratio  $R_{b\tau}(t) = \sqrt{\frac{Y_b(t)}{Y_\tau(t)}}$  of the Yukawa couplings for the  $b$ -quark and the  $\tau$ -lepton,

$$\frac{dR_{b\tau}}{dt} = -R_{b\tau} \left( \frac{1}{2}Y_t - \frac{8}{3}\tilde{\alpha}_3 + \frac{2}{3}\tilde{\alpha}_1 \right),
\tag{25}$$

where  $Y_b = \left(\frac{h_b(t)}{4\pi}\right)^2$  and  $Y_\tau(t) = \left(\frac{h_\tau(t)}{4\pi}\right)^2$ . The value of  $R_{b\tau}(0) = 1$  corresponds to the unification of the Yukawa couplings  $h_b$  and  $h_\tau$ . For the Yukawa and gauge couplings the set of two-loop renormalisation group equations within the NMSSM is presented in [30].

The corresponding one-loop equations for the gauge couplings can easily be integrated. The result has the form:

$$\tilde{\alpha}_i(t) = \frac{\tilde{\alpha}_i(0)}{1 + b_i\tilde{\alpha}_i(0)t}.
\tag{26}$$

Since the gauge couplings within the MSSM and within the NMSSM coincide at the Grand Unification scale, we have  $\tilde{\alpha}_i(0) = \tilde{\alpha}(0) = \tilde{\alpha}_{\text{GUT}}$  for all of them. In the case where  $\lambda = 0$ , there exists an exact analytic solution to the set of renormalisation group

equations (24). It is specified by relations (2) and (8), with  $E(t)$  and  $F(t)$  being given by

$$\begin{aligned}
H(t) &= \frac{16}{3}\tilde{\alpha}_3(t) + 3\tilde{\alpha}_2(t) + \frac{13}{15}\tilde{\alpha}_1(t), \\
E(t) &= \exp \left[ \int_0^t H(t') dt' \right] = \left[ \frac{\tilde{\alpha}_3(t)}{\tilde{\alpha}(0)} \right]^{16/9} \left[ \frac{\tilde{\alpha}_2(t)}{\tilde{\alpha}(0)} \right]^{-3} \left[ \frac{\tilde{\alpha}_1(t)}{\tilde{\alpha}(0)} \right]^{-13/99}, \\
F(t) &= \int_0^t E(t') dt'.
\end{aligned} \tag{27}$$

In the regime of strong Yukawa coupling, in which case all  $Y_i(0)$  are much greater than  $\tilde{\alpha}(0)$ , an exact analytic solution to the set of Eqs.(24) has not yet been found. An explicit  $t$  dependence of the Yukawa couplings can be obtained on the basis of an approximate solution to the renormalisation group equations within the NMSSM. An approximate solution of this type was first obtained by Kazakov [37], who studied the renormalisation group equations within the MSSM in the limit  $\tan\beta \gg 1$ . For the Yukawa couplings, it has the form:

$$\begin{aligned}
Y_\lambda(t) &= Y_\lambda(0)E_\lambda(t)P_2(t)P_1(t)P_Y(t), \\
Y_\varkappa(t) &= Y_\varkappa(0)P_Y^3(t), \\
Y_t(t) &= Y_t(0)E_t(t)P_Q(t)P_U(t)P_2(t),
\end{aligned} \tag{28}$$

where

$$E_t(t) = E(t), \quad E_\lambda(t) = \left( \frac{\tilde{\alpha}_2(t)}{\tilde{\alpha}(0)} \right)^{-3} \left( \frac{\tilde{\alpha}_1(t)}{\tilde{\alpha}(0)} \right)^{-1/11},$$

and  $P_i(t)$  is the contribution of the Yukawa couplings to the renormalisation of  $Y_i(t)$  from each of the external legs entering the corresponding vertex:

$$\begin{aligned}
\frac{d \ln P_Q(t)}{dt} &= \frac{1}{2} \frac{d \ln P_U(t)}{dt} = -Y_t(t), & \frac{d \ln P_2(t)}{dt} &= -3Y_t(t) - Y_\lambda(t), \\
\frac{d \ln P_1(t)}{dt} &= -Y_\lambda(t), & \frac{d \ln P_Y(t)}{dt} &= -2Y_\lambda(t) - 2Y_\varkappa(t).
\end{aligned} \tag{29}$$

Setting  $P_Q(t)P_U(t)P_2(t) \approx P_2(t)P_1(t)P_Y(t) \approx P_Y^3(t) \approx P_0(t)$  and  $P_Q^A(t) \approx P_U^B(t) \approx P_2^{C_2}(t) \approx P_1^{C_1}(t) \approx P_Y^D(t) \approx P_0(t)$ , we find that  $A$ ,  $B$ ,  $C_1$ ,  $C_2$ , and  $D$  satisfy the relations:

$$\frac{1}{A} + \frac{1}{B} + \frac{1}{C_2} = 1, \quad \frac{1}{D} + \frac{1}{C_1} + \frac{1}{C_2} = 1, \quad D = 3.$$

Since the contribution of the  $t$ -quark Yukawa coupling to the renormalisation of external legs is much greater than the contribution of  $Y_\lambda$ , the constants  $A$ ,  $B$ , and  $C_2$  also satisfy the approximate relations  $B \approx A/2$  and  $C_2 \approx A/3$ , which make it possible to find, for  $A$ ,  $B$ ,  $C_1$ , and  $C_2$ , that

$$A = C_1 = 6, \quad B = 3, \quad C_2 = 2$$

and to obtain, with the aid of the differential equations (29) for  $P_i(t)$ , approximate solutions for the latter quantities. The results are

$$\begin{aligned}
P_U(t) &= \frac{1}{(1 + 6Y_t(0)F_t(t))^{1/3}} = P_Q^2(t), \\
P_{H_2}(t) &= \frac{1}{(1 + 6Y_t(0)F_t(t) + 2Y_\lambda(0)F_\lambda(t))^{1/2}}, \\
P_{H_1}(t) &= \frac{1}{(1 + 6Y_\lambda(0)F_\lambda(t))^{1/6}}, \\
P_Y(t) &= \frac{1}{(1 + 6Y_\lambda(0)F_\lambda(t) + 6Y_\varkappa(0)t)^{1/3}},
\end{aligned} \tag{30}$$

where

$$F_t(t) = F(t), \quad F_\lambda(t) = \int_0^t E_\lambda(t') dt'.$$

Substituting the resulting expressions (30) for  $P_i(t)$  into relations (28), we obtain approximate solutions for the Yukawa couplings within the NMSSM. In just the same way, we can find approximate solutions for  $Y_t(t)$  and  $Y_\lambda(t)$  at  $\varkappa = 0$ . As a result, it can easily be proven that the required solutions are obtained by setting  $Y_\varkappa(0) = 0$  in (28) and (30).

**Table.** Values of the Yukawa couplings at the electroweak scale for various initial values  $\varkappa^2(0)$ ,  $\lambda^2(0)$ , and  $h_t^2(0)$ .

$\varkappa^2(0)$	$\lambda^2(0)$	$h_t^2(0)$	$\varkappa^2(t_0)$	$\lambda^2(t_0)$	$h_t^2(t_0)$	$h_t^2(t_0) + 0.51\lambda^2(t_0)$	$h_t^2(t_0) + 0.72\lambda^2(t_0) + 0.33\varkappa^2(t_0)$
0	10	10	0	0.3220	1.1538	1.3180	1.3857
0	6	10	0	0.2879	1.1675	1.3143	1.3747
0	2	10	0	0.1911	1.1987	1.2962	1.3363
0	10	6	0	0.3492	1.1327	1.3108	1.3841
0	6	6	0	0.3167	1.1475	1.3090	1.3755
0	2	6	0	0.2203	1.1815	1.2939	1.3402
0	10	2	0	0.4209	1.0513	1.2659	1.3543
0	6	2	0	0.3901	1.0715	1.2704	1.3524
0	2	2	0	0.2941	1.1160	1.2660	1.3277
10	10	10	0.1480	0.2480	1.1737	1.3002	1.4011
10	6	10	0.1995	0.1969	1.1904	1.2908	1.3980
10	2	10	0.2956	0.0979	1.2193	1.2692	1.3874
10	10	6	0.1256	0.2801	1.1527	1.2956	1.3958
10	6	6	0.1760	0.2279	1.1712	1.2875	1.3934
10	2	6	0.2785	0.1192	1.2047	1.2655	1.3825
10	10	2	0.0865	0.3601	1.0734	1.2570	1.3612
10	6	2	0.1305	0.3060	1.0984	1.2545	1.3618
10	2	2	0.2385	0.1775	1.1458	1.2363	1.3523
2	10	10	0.0655	0.2941	1.1608	1.3108	1.3942
2	6	10	0.1055	0.2482	1.1767	1.3033	1.3903
2	2	10	0.2059	0.1396	1.2092	1.2804	1.3777
2	10	6	0.0521	0.3244	1.1395	1.3049	1.3903
2	6	6	0.0875	0.2798	1.1567	1.2994	1.3870
2	2	6	0.1865	0.1663	1.1929	1.2778	1.3742
2	10	2	0.0322	0.4007	1.0582	1.2625	1.3573
2	6	2	0.0578	0.3581	1.0810	1.2637	1.3580
2	2	2	0.1464	0.2361	1.1297	1.2501	1.3480

## References

- [1] R. Tallach, Nucl. Phys. B **183**, 384 (1981); S. Narison, Phys. Lett. B **197**, 405 (1987); N. Gray, D. J. Broadhurst, W. Grafe, and K. Schilcher, Z. Phys. C **48**, 673 (1990).
- [2] M. Jones, in *Proceedings of the XXXIIIrd Recontres de Moriond on Electroweak Interactions and Unified Theories, Les Arcs, France, 1998*, in press.
- [3] L. E. Ibañez and C. Lopez, Phys. Lett. B **126**, 54 (1983); L. E. Ibañez and C. Lopez, Nucl. Phys. B **233**, 511 (1984); W. De Boer, R. Ehret, and D. I. Kazakov, Z. Phys. C **67**, 647 (1995).
- [4] C. T. Hill, Phys. Rev. D **24**, 691 (1981); C. T. Hill, C. N. Leung, and S. Rao, Nucl. Phys. B **262**, 517 (1985).
- [5] B. Pendleton and G. G. Ross, Phys. Lett. B **98**, 291 (1981); D. I. Kazakov, JINR Preprint E2-82-880, 1982; M. Lanzagorta and G. G. Ross, Phys. Lett. B **349**, 319 (1995); **364**, 163 (1995); M. Bando, J. Sato, and K. Yoshioka, Prog. Theor. Phys. **98**, 169 (1997); B. C. Allanach, G. Amelino-Camelia, and O. Philipsen, Phys. Lett. B **393**, 349 (1997).
- [6] B. C. Allanach and S. F. King, Phys. Lett. B **407**, 124 (1997); I. Jack and D. R. T. Jones, Phys. Lett. B **443**, 177 (1998).
- [7] B. Schrempp, Phys. Lett. B **344**, 193 (1995).
- [8] S. A. Abel and B. C. Allanach, Phys. Lett. B **415**, 71 (1997).
- [9] P. M. Ferreira, I. Jack, and D. R. T. Jones, Phys. Lett. B **392**, 376 (1997).
- [10] B. Brahmachari, Mod. Phys. Lett. A **12**, 1969 (1997).
- [11] J. A. Casas, J. R. Espinosa, and H. E. Haber, Nucl. Phys. B **526**, 3 (1998).
- [12] G. K. Yeghiyan, M. Jurčišin, and D. I. Kazakov, Mod. Phys. Lett. A **14**, 601 (1999).
- [13] S. Codoban, M. Jurčišin, and D. Kazakov, hep-ph/9912504.
- [14] M. Carena, M. Olechowski, S. Pokorski, and C. E. M. Wagner, Nucl. Phys. B **419**, 213 (1994); M. Carena and C. E. M. Wagner, Nucl. Phys. B **452**, 45 (1995).
- [15] V. Barger, M. S. Berger, P. Ohmann, and J. N. Phillips, Phys. Lett. B **314**, 351 (1993); W. A. Bardeen, M. Carena, S. Pokorski, and C. E. M. Wagner, Phys. Lett. B **320**, 110 (1994); S. A. Abel and B. C. Allanach, Phys. Lett. B **431**, 339 (1998).
- [16] V. Barger, M. S. Berger, and P. Ohmann, Phys. Rev. D **49**, 4908 (1994).
- [17] M. S. Chanowitz, J. Ellis, and M. K. Gaillard, Nucl. Phys. B **128**, 506 (1977); A. J. Buras, J. Ellis, M. K. Gaillard, and D. V. Nanopoulos, Nucl. Phys. B **135**, 66 (1978).

- [18] V. Barger, M. S. Berger, and P. Ohmann, Phys. Rev. D **47**, 1093 (1993); M. Carena, S. Pokorski, and C. E. M. Wagner, Nucl. Phys. B **406**, 59 (1993); P. Langacker and N. Polonsky, Phys. Rev. D **49**, 1454 (1994); **50**, 2199 (1994); N. Polonsky, Phys. Rev. D **54**, 4537 (1996).
- [19] M. Carena, M. Olechowski, S. Pokorski, and C. E. M. Wagner, Nucl. Phys. B **426**, 269 (1994);
- [20] B. Schrempp and M. Wimmer, Prog. Part. Nucl. Phys. **37**, 1 (1996);
- [21] E. Gross, in *Proceedings of International Europhysics Conference on High Energy Physics, Tampere, Finland, 1999*, in press.
- [22] M. Jurčišin and D. I. Kazakov, Mod. Phys. Lett. A **14**, 671 (1999).
- [23] P. Fayet, Nucl. Phys. B **90**, 104 (1975); M. I. Vysotsky and K. A. Ter-Martirosyan, Sov. Phys. – JETP **63**, 489 (1986).
- [24] J. Ellis, J. F. Gunion, H. E. Haber, L. Roszkowski, and F. Zwirner, Phys. Rev. D **39**, 844 (1989).
- [25] L. Durand and J. L. Lopes, Phys. Lett. B **217**, 463 (1989); L. Drees, Int. J. Mod. Phys. A **4**, 3635 (1989).
- [26] M. Masip, R. Muñoz-Tapia, and A. Pomarol, Phys. Rev. D **57**, 5340 (1998); G. K. Yeghiyan, YERPHI Preprint YERPHI-1532(2)-99, 1999; hep-ph/9904488; U. Ellwanger and C. Hugonie, hep-ph/9909260.
- [27] H. E. Haber and R. Hempfling, Phys. Rev. Lett. **66**, 1815 (1991); Y. Okada, M. Yamaguchi, and T. Yanagida, Prog. Theor. Phys. **85**, 1 (1991); J. Ellis, G. Ridolfi, and F. Zwirner, Phys. Lett. B **257**, 83 (1991); **262**, 477 (1991); R. Barbieri, M. Frigeni, and F. Caravaglios, Phys. Lett. B **258**, 167 (1991); Y. Okada, M. Yamaguchi, and T. Yanagida, Phys. Lett. B **262**, 54 (1991); M. Drees and M. Nojiri, Phys. Rev. D **45**, 2482 (1992); D. M. Pierce, A. Papadopoulos, and S. Jhonson, Phys. Rev. Lett. **68**, 3678 (1992); P. H. Chankowski, S. Pokorski, and J. Rosiek, Phys. Lett. B **274**, 191 (1992); H. E. Haber and R. Hempfling, Phys. Rev. D **48**, 4280 (1993); P. H. Chankowski, S. Pokorski, and J. Rosiek, Nucl. Phys. B **423**, 437 (1994); A. Yamada, Z. Phys. C **61**, 247 (1994); A. Dabelstein, Z. Phys. C **67**, 495 (1995); D. M. Pierce, J. A. Bagger, K. Matchev, and R. Zhang, Nucl. Phys. B **491**, 3 (1997).
- [28] J. R. Espinosa and M. Quiros, Phys. Lett. B **266**, 389 (1991); R. Hempfling and A. H. Hoang, Phys. Lett. B **331**, 99 (1994); M. Carena, J. R. Espinosa, M. Quiros, and C. E. M. Wagner, Phys. Lett. B **355**, 209 (1995); J. A. Casas, J. R. Espinosa, M. Quiros, and A. Riotto, Nucl. Phys. B **436**, 3 (1995); M. Carena, M. Quiros, and C. E. M. Wagner, Nucl. Phys. B **461**, 407 (1996); H. E. Haber, R. Hempfling, and A. H. Hoang, Z. Phys. C **75**, 539 (1997); S. Heinemeyer, W. Hollik, and G. Weiglein, Phys. Rev. D **58**, 091701 (1998); Phys. Lett. B **440**, 296 (1998); R. Zhang, Phys. Lett. B **447**, 89 (1999); S. Heinemeyer, W. Hollik, and G. Weiglein, Phys. Lett. B **455**, 179 (1999).

- [29] T. Elliott, S. F. King, and P. L. White, Phys. Lett. **319**, 56 (1993); U. Ellwanger, Phys. Lett. B **303**, 271 (1993); U. Ellwanger and M. Lindner, Phys. Lett. B **301**, 365 (1993); P. N. Pandita, Phys. Lett. B **318**, 338 (1993); P. N. Pandita, Z. Phys. C **59**, 575 (1993); T. Elliott, S. F. King, and P. L. White, Phys. Rev. D **49**, 2435 (1994); S. W. Ham, S. K. Oh, and B. R. Kim, J. Phys. G **22**, 1575 (1996); Phys. Lett. B **414**, 305 (1997); P. A. Kovalenko, R. B. Nevzorov, and K. A. Ter-Martirosyan, Phys. Atom. Nucl. **61**, 812 (1998).
- [30] S. F. King and P. L. White, Phys. Rev. D **52**, 4183 (1995).
- [31] S. W. Ham, S. K. Oh, and H. S. Song, hep-ph/9910461.
- [32] A. Pomarol, Phys. Rev. D **47**, 273 (1993); K. S. Babu and S. M. Barr, Phys. Rev. D **49**, 2156 (1994); G. M. Asatrian and G. K. Egian, Mod. Phys. Lett. A **10**, 2943 (1995); **11**, 2771 (1996); N. Haba, M. Matsuda, and M. Tanimoto, Phys. Rev. D **54**, 6928 (1996).
- [33] M. A. Diaz, T. A. Ter Veldius, and T. J. Weiler, Phys. Rev. D **54**, 5855 (1996).
- [34] J. – P. Derendinger and C. A. Savoy, Nucl. Phys. B **237**, 307 (1984).
- [35] P. Binetruy and C. A. Savoy, Phys. Lett. B **277**, 453 (1992).
- [36] B. Schrempp and F. Schrempp, Phys. Lett. B **299**, 321 (1993).
- [37] S. Codoban and D. I. Kazakov, hep-ph/9906256.
- [38] B. C. Allanach and S. F. King, Phys. Lett. B **328**, 360 (1994).

# Figure captions

**Fig.1.** Boundary conditions for the renormalisation group equations of the NMSSM at the scale  $q = M_X$  for  $\varkappa^2 = 0$  uniformly distributed in the  $(\rho_t, \rho_\lambda)$  plane in a square  $2 \leq h_t^2(0), \lambda^2(0) \leq 10$  – Fig.1a, and the corresponding values of the Yukawa couplings at the electroweak scale – Fig.1b. The thick and thin curves in Fig.1b represent, respectively, the invariant and the Hill line. The dashed line in Fig.1b is a fit of the values  $(\rho_t(t_0), \rho_\lambda(t_0))$  for  $20 \leq h_t^2(0), \lambda^2(0) \leq 100$ .

**Fig.2.** Boundary conditions for the renormalisation group equations of the NMSSM at the scale  $q = M_X$  for  $\varkappa^2 = 0$  uniformly distributed in the  $(\rho_t, \rho_\lambda)$  plane in a square  $20 \leq h_t^2(0), \lambda^2(0) \leq 100$  – Fig.2a, and the corresponding values of the Yukawa couplings at the electroweak scale – Fig.2b. The thick and thin curves in Fig.2b represent, respectively, the invariant and the Hill line. The dashed line in Fig.2b is a fit of the values  $(\rho_t(t_0), \rho_\lambda(t_0))$  for  $20 \leq h_t^2(0), \lambda^2(0) \leq 100$ .

**Fig.3.** Evolution of the combination  $\rho_t(t) + 0.506\rho_\lambda(t)$  of the Yukawa couplings from the Grand Unification scale ( $t = 0$ ) to the electroweak scale ( $t = t_0$ ) for  $\varkappa^2 = 0$  and for various initial values  $h_t^2(0)$  – Fig.3a,  $\lambda^2(0)$  – Fig.3b.

**Fig.4.** Boundary conditions for the renormalisation group equations of the NMSSM at the scale  $q = M_X$  for  $\lambda^2 = 0$  uniformly distributed in the  $(\rho_t, \rho_\varkappa)$  plane in a square  $2 \leq h_t^2(0), \varkappa^2(0) \leq 10$  – Fig.4a, and the corresponding values of the Yukawa couplings at the electroweak scale – Fig.4b. The thick and thin curves in Fig.4b represent, respectively, the invariant and the Hill line.

**Fig.5.** Quasi-fixed surface in the  $(\rho_t, \rho_\varkappa, \rho_\lambda)$  space. The shaded part of the surface represents the region near which the solutions corresponding to the initial values  $2 \leq h_t^2(0), \varkappa^2(0), \lambda^2(0) \leq 10$  – Fig.5a,  $20 \leq h_t^2(0), \varkappa^2(0), \lambda^2(0) \leq 100$  – Fig.5b are concentrated.

**Fig.6.** Evolution of the combination  $\rho_t + 0.720\rho_\lambda + 0.3330\rho_\varkappa$  of the Yukawa couplings from the Grand Unification scale ( $t = 0$ ) to the electroweak scale ( $t = t_0$ ) for various initial values  $h_t^2(0)$  – Fig.6a,  $\lambda^2(0)$  – Fig.6b,  $\varkappa^2(0)$  – Fig.6c.

**Fig.7.** Invariant and quasi-fixed lines in the  $(\rho_t, \rho_\lambda)$  plane obtained by means of numerical calculations (thick and thin solid curves) and by means of approximate solution of the renormalisation group equations of the NMSSM (dashed and dotted curves). The thick solid curve and the dashed curve represent the infrared fixed line, while the thin solid curve and the dotted curve represent the Hill line.

**Fig.8.** The values of the Yukawa couplings at the electroweak scale corresponding to the unification of  $h_b$  and  $h_\tau$  at the scale  $q = M_X$  (thick line). The infrared quasi-fixed line is also presented here (thin line).



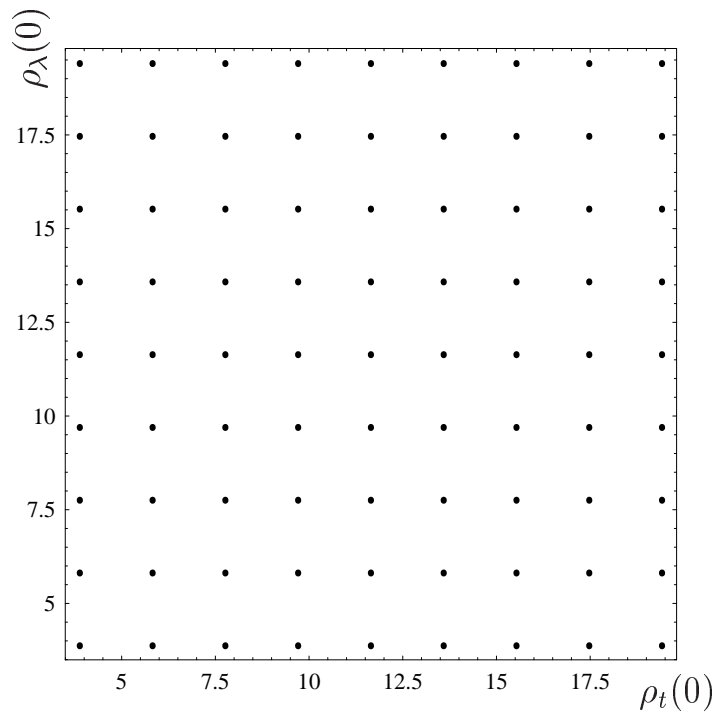


Fig.1a.

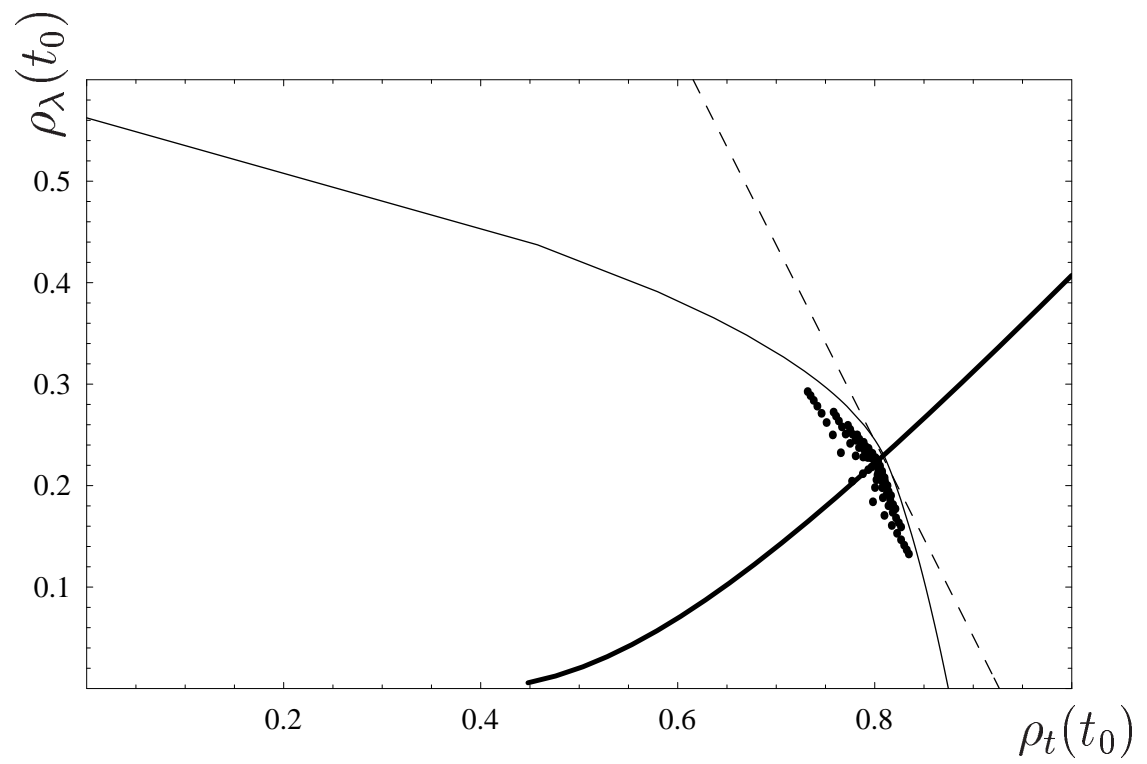


Fig.1b.

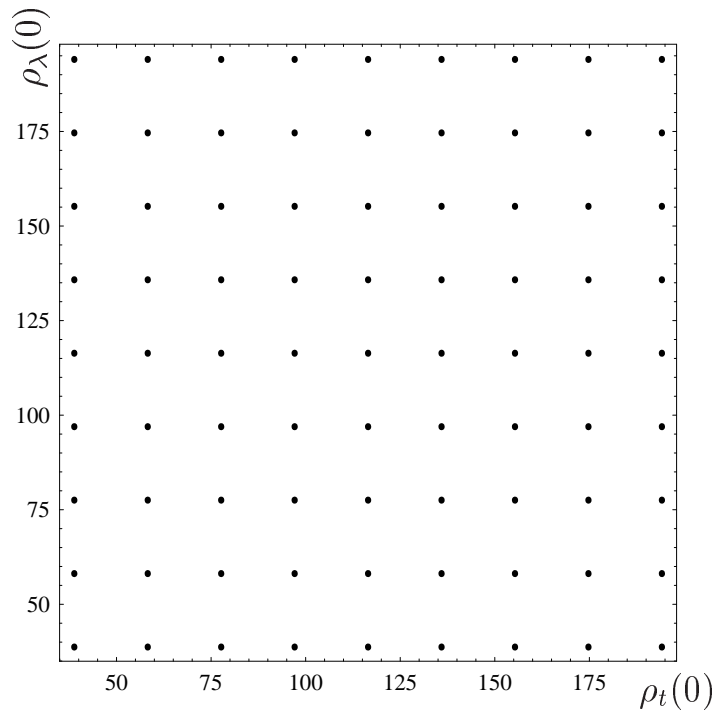


Fig.2a.

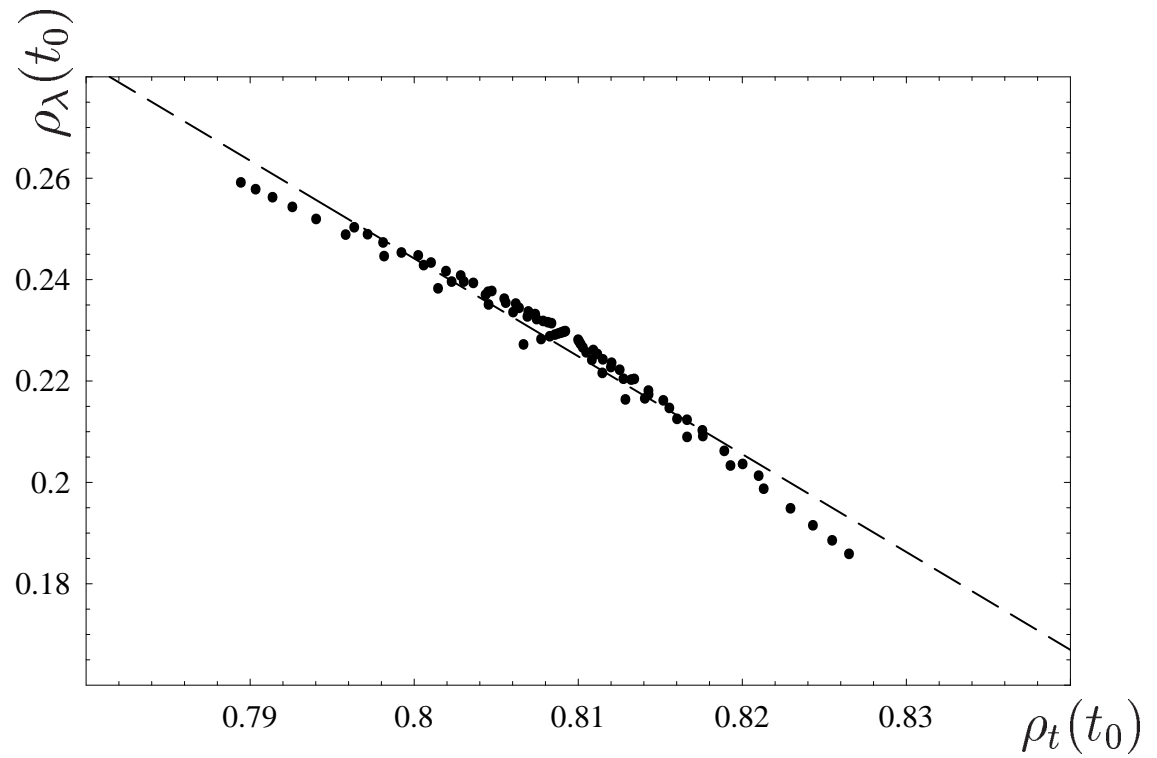


Fig.2b.

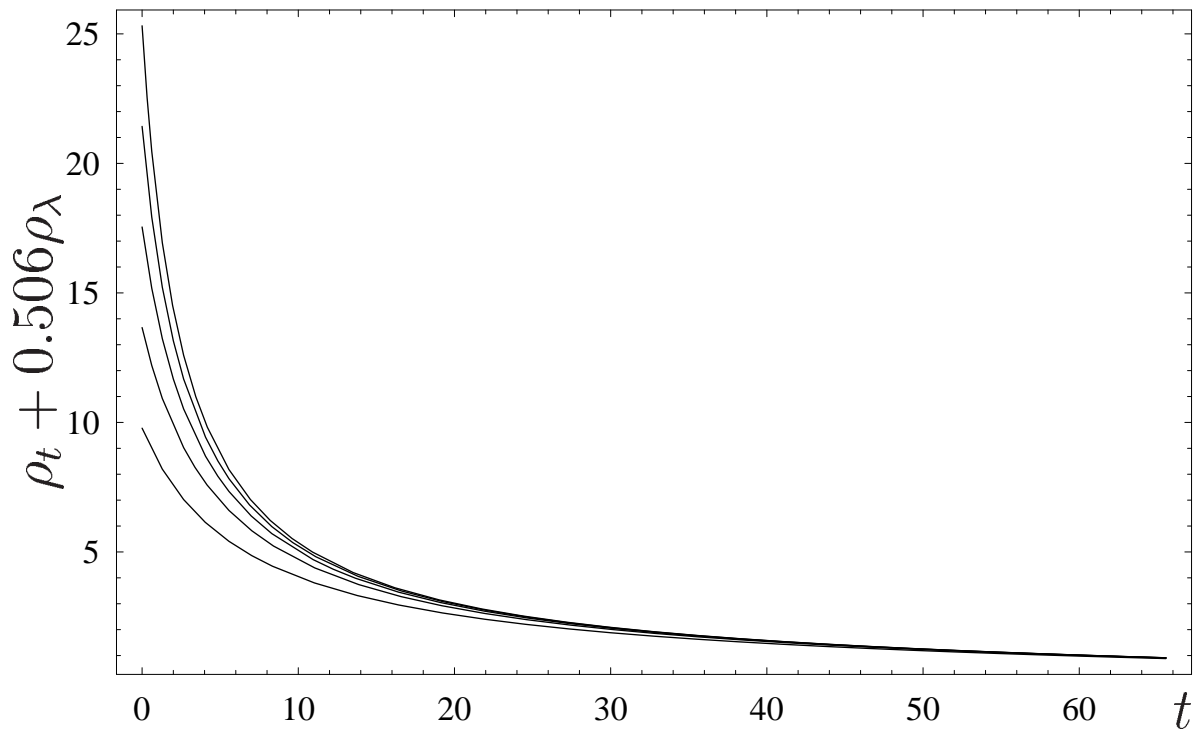


Fig.3a.

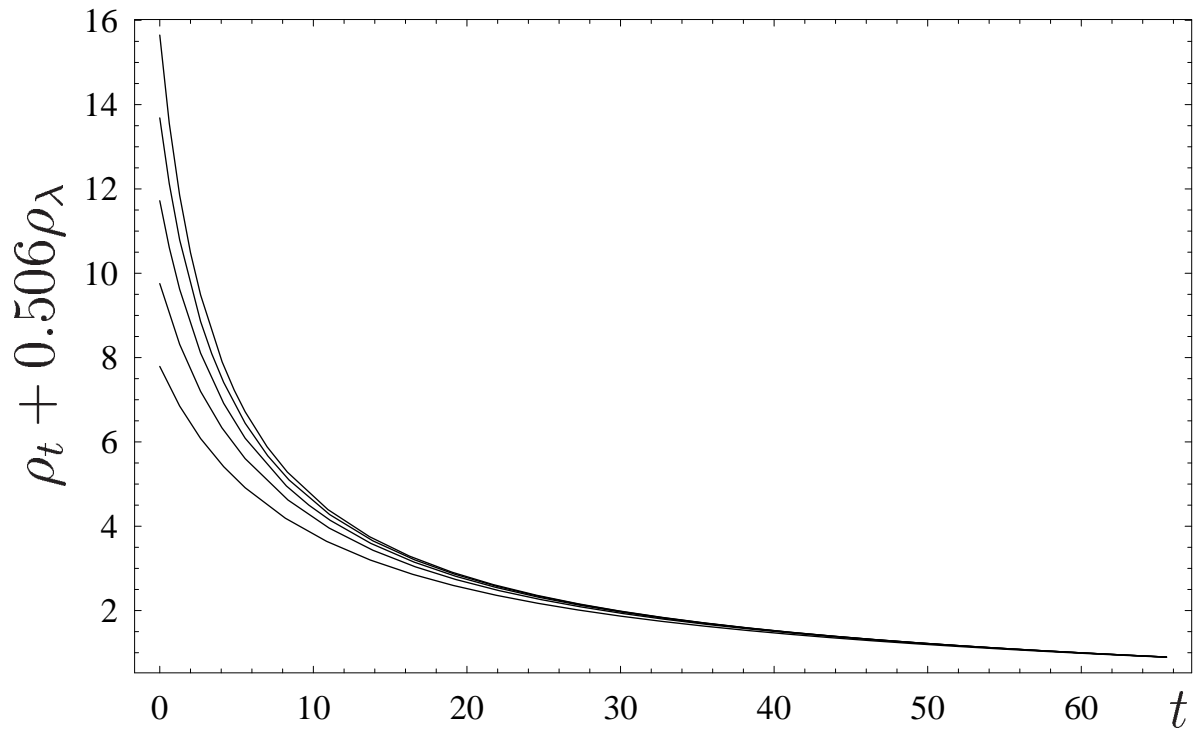


Fig.3b.

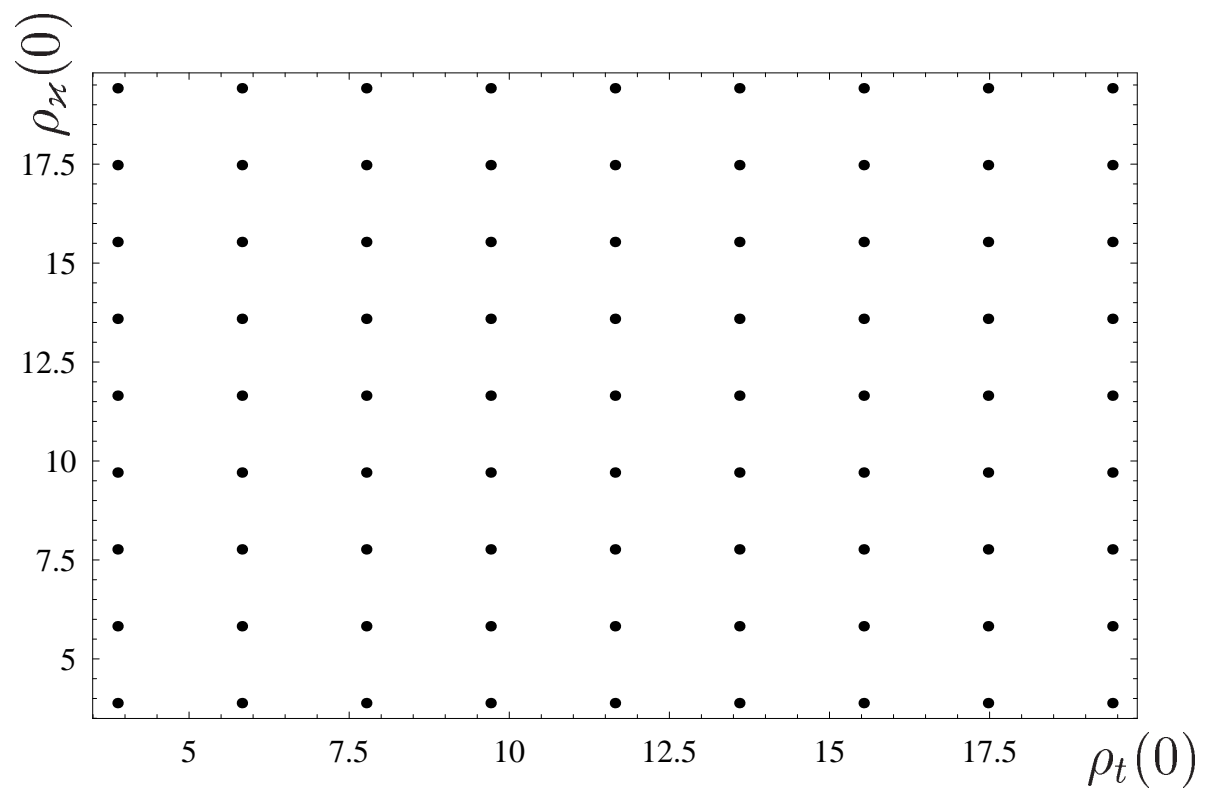


Fig.4a.

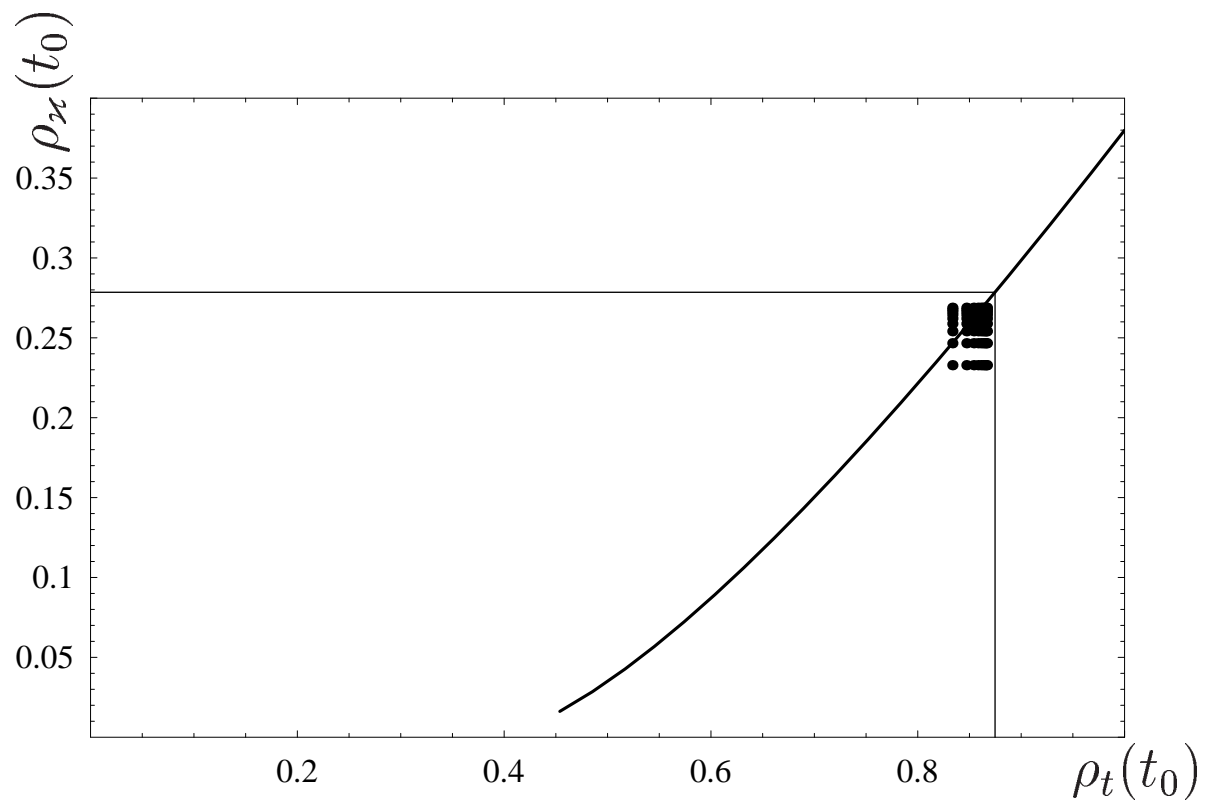


Fig.4b.

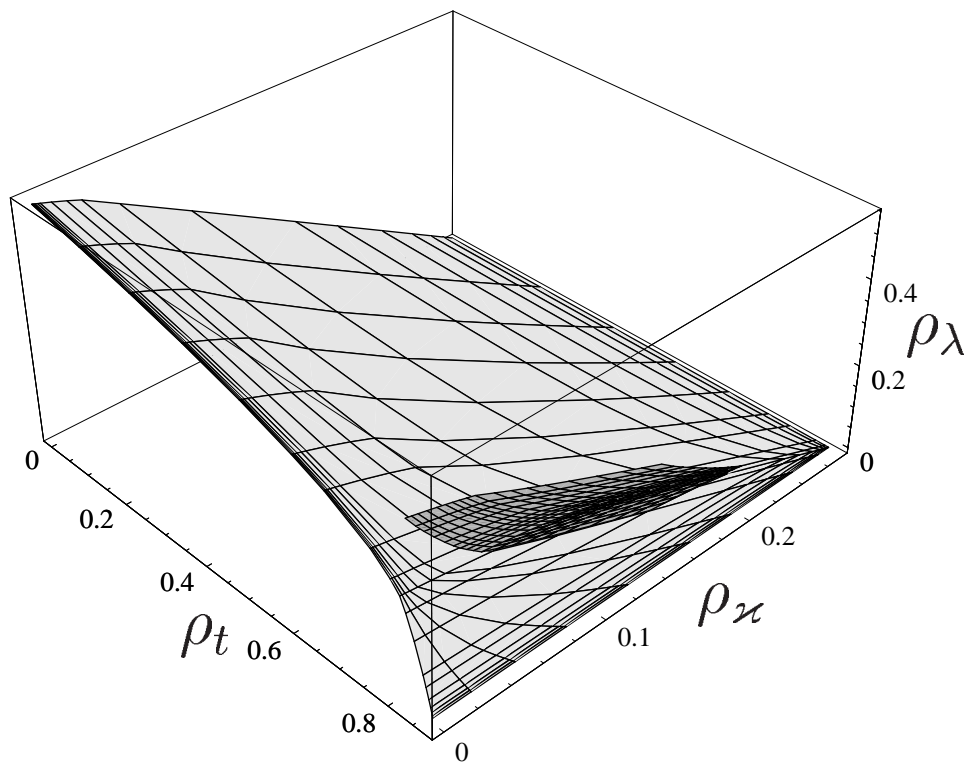


Fig.5a.

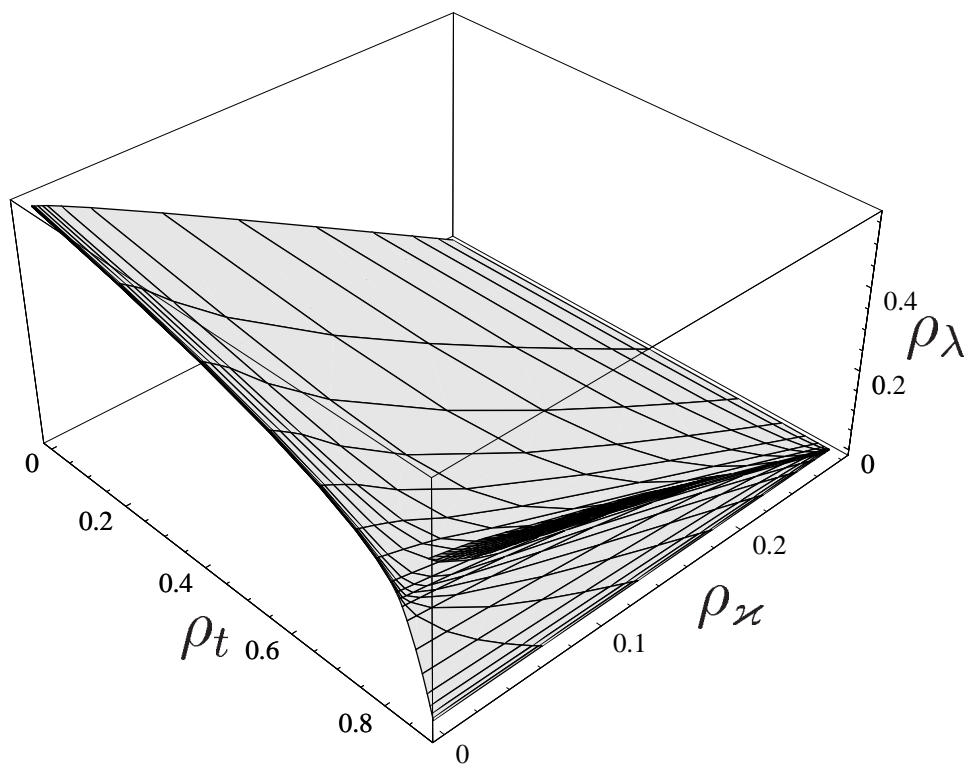
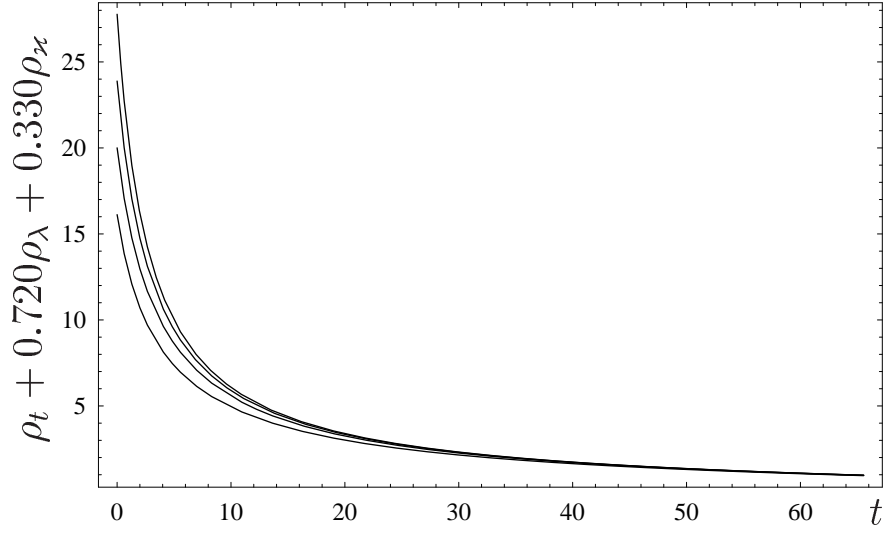
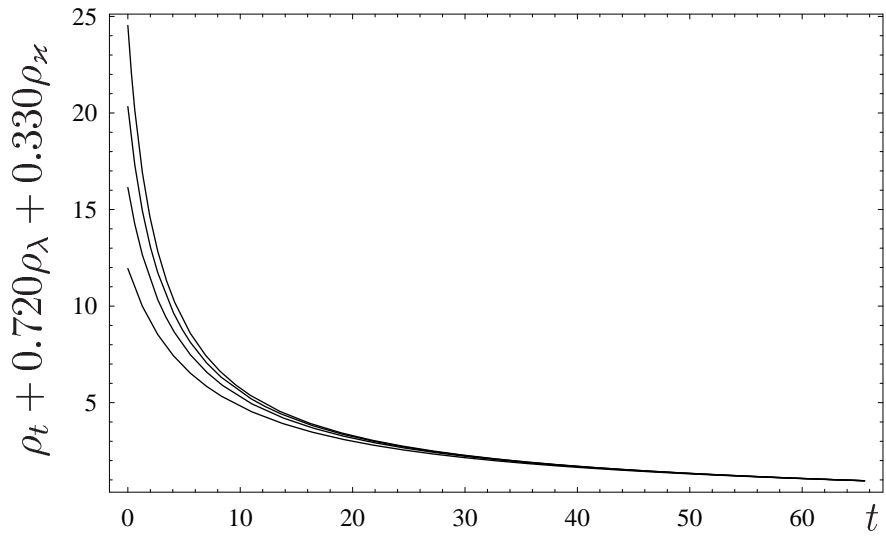


Fig.5b.



**Fig.6a.**



**Fig.6b.**

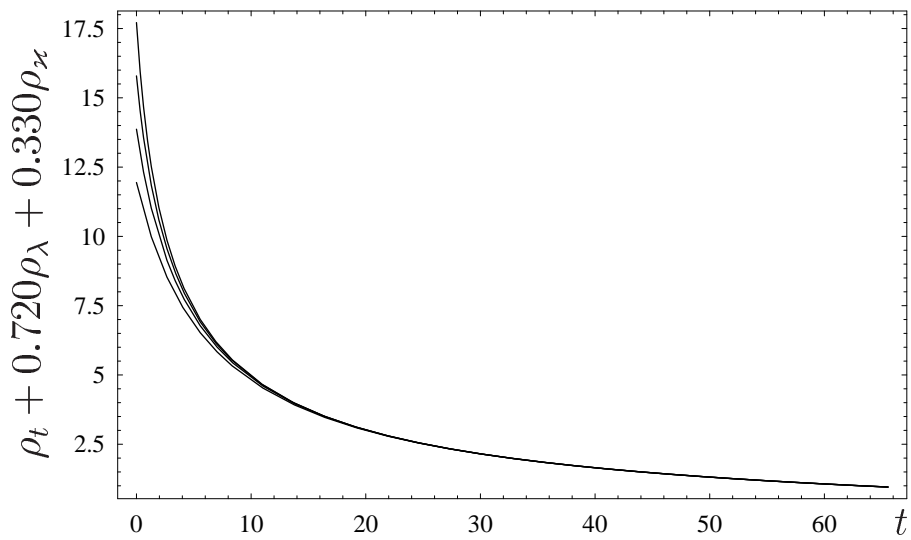


**Fig.6c.**

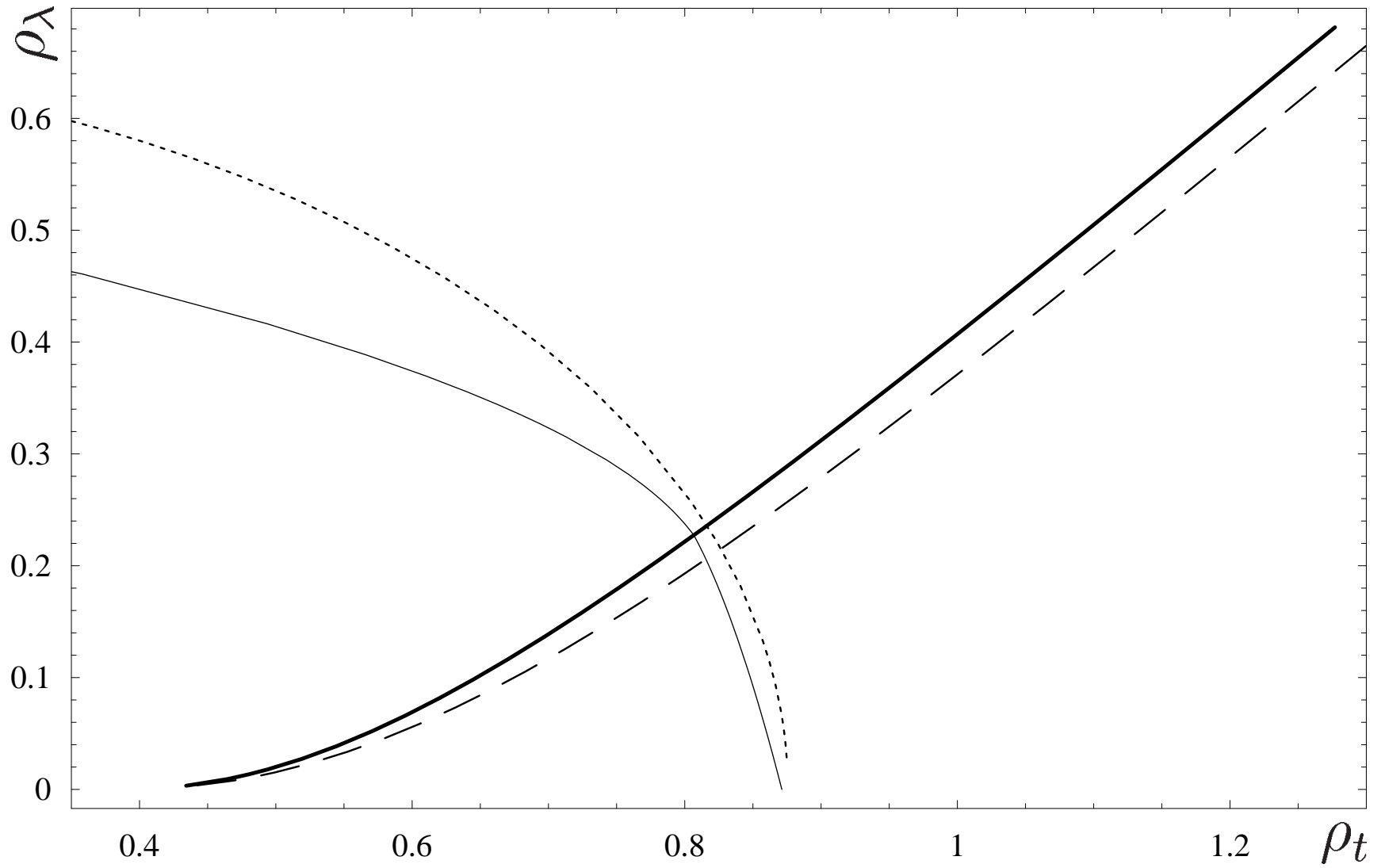


Fig.7.

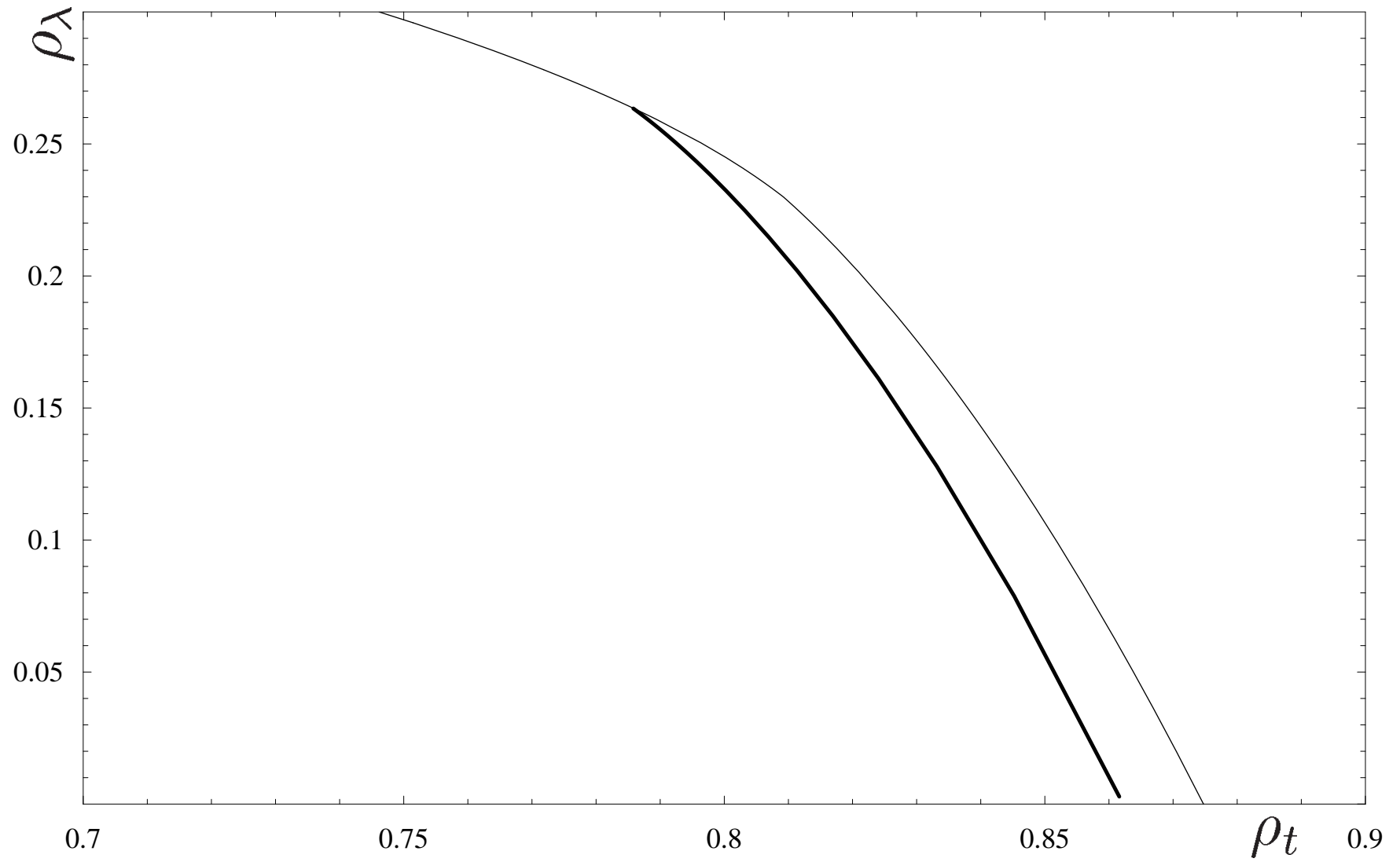


Fig.8.